Research Square

Preprints are preliminary reports that have not undergone peer review.
They should not be considered conclusive, used to inform clinical practice,
or referenced by the media as validated information.

Hydro-Economic-Environmental Trade-offs in Climate Adaptation: Optimizing Agricultural Resource Allocation in Arid Regions

Elahe Ahani
Zabol University
Saman Ziaee
Zabol University
Hamid Mohammadi
Zabol University
Mostafa Mardani Najafabadi
m.mardani@asnrukh.ac.ir

Agricultural Sciences and Natural Resources University of Khuzestan
Abbas Mirzaei
Agricultural Sciences and Natural Resources University of Khuzestan

Research Article

Keywords: Food Security, Climate Change, Farmer Adaptation, Optimization, Agricultural Planning

Posted Date: June 30th, 2026

DOI: https://doi.org/10.21203/rs.3.rs-9549111/v1

License: This work is licensed under a Creative Commons Attribution 4.0 International License.
Read Full License

Additional Declarations: No competing interests reported.

Hydro-Economic-Environmental Trade-offs in Climate Adaptation: Optimizing Agricultural Resource Allocation in Arid Regions

Abstract

Climate change intensifies pressure on already scarce water resources in arid agricultural systems, threatening food security, farmer livelihoods, and environmental sustainability. This paper develops an integrated hydro-economic-environmental modeling framework to evaluate climate adaptation strategies that jointly address economic efficiency, water conservation, and greenhouse gas mitigation in Iran's Kashafrud River Basin—a representative arid region facing acute water stress. Using a multi-objective optimization model grounded in the Water–Energy–Food (WEF) nexus, we simulate farmer responses under the high-emissions SSP5 scenario (2021–2040). Without intervention, climate change reduces cultivated area by 39% and farmer profits by 24%. However, a nexus-based adaptation policy—combining optimized crop allocation with a 10% improvement in irrigation efficiency—reverses this trend: cultivated area expands by 15%, gross profits increase by 8%, and GHG emissions fall by 44%. The results demonstrate that economically viable and environmentally sound adaptation is achievable through coordinated resource reallocation that prioritizes crops with high profit-to-water and low carbon footprints. Our modular, data-driven approach offers a scalable template for policy design in water-scarce regions worldwide, aligning with the goals of sustainable development and climate-resilient agriculture.

Keywords: Food Security, Climate Change, Farmer Adaptation, Optimization, Agricultural Planning

1 Introduction

According to the scientific consensus, the Earth's climate has undergone significant disruptions as a result of human economic activities, particularly the release of greenhouse gases into the atmosphere. This increase in greenhouse gas concentrations has precipitated two notable phenomena: global warming and climate change (Wang et al., 2023). This phenomenon has precipitated alterations in river flows, groundwater aquifers, and the supply of water required for agriculture, drinking, and industry. According to the most recent classification by the International Geographical Organization, Iran is categorized among arid and semi-arid regions in terms of climate (Kalbali et al., 2021).

The evaporation rate of rainfall in Iran during the 2017-2018 water year averaged 2,700 millimeters, while the global average is approximately 800 millimeters. In essence, the nation undergoes evaporation that is equivalent to one-third of the global precipitation, and three times the global evaporation rate. This finding suggests that Iran is facing severe water resource scarcity (Ikram et al., 2020; Madani et al., 2016). Agriculture is the dominant water user in Iran, accounting for approximately 92% of total water withdrawals, compared to 6% for

industrial and 2% for domestic purposes (FAO, 2008). This high dependency, coupled with prevailing irrigation inefficiencies, results in agricultural water use intensity that substantially exceeds global averages. It is evident that the manner in which water resources or groundwater aquifers are utilized in the agricultural, drinking, sanitation, and industrial sectors plays a significant role in the productivity and efficiency of per capita renewable water. Despite comprising 1.3% of the global population, Iran's allocation of freshwater resources is a mere 0.2%, a disproportionate share that highlights the country's water scarcity challenges. Consequently, demand for water, food, and energy has increased in recent decades due to population growth and migration, economic development, international trade, urbanization, cultural and technological changes, and climate change (Emamzadeh et al., 2016; Nabavi-Pelesaraei et al., 2016).

Agricultural economists have frequently examined and analyzed climate change based on its impact on farmers' income or the welfare and economic surplus of this sector. It is imperative to acknowledge that, despite the substantial financial investments required to adapt agricultural sectors (Motta et al., 2025), the efficacy of certain adaptation strategies remains to be fully elucidated. Nevertheless, information can function as a pivotal element in fostering of the agricultural sector. The phenomenon of climate change has had a profound impact on the availability of water resources. Given the foundational role of water in socio-economic development and the interconnected nature of these systems, these changes are anticipated to adversely impact these sectors and precipitate systemic instability in the future (Motta et al., 2025; Esteve et al., 2015). In light of these circumstances, the attainment of systemic resilience has emerged as a global objective, guided by strategies aimed at mitigating the vulnerability of systems across all sectors in the face of such changes. Consequently, the assessment of climate change impacts to develop adaptation strategies, and the subsequent evaluation of these strategies using mathematical programming methods, is imperative (Kurian, 2017).

In this regard, a considerable body of research has been conducted, the majority of which have focused on examining a single system, such as groundwater resources, surface water resources, agriculture, etc. However, it is important to note that different systems interact with and influence each other. These intersectoral interactions play a crucial role in the vulnerability in overall system and must be considered when evaluating strategies to reduce its vulnerability (Wu et al., 2022). Consequently, focused assessments that emphasize only one sector are inadequate for comprehensively understanding the system, the impacts of climate change on it, and adaptation strategies. This is due to their inability to capture the relationships and dynamics within the system.

Furthermore, within any system, certain processes inevitably evolve over time, giving rise to unintended consequences. These consequences impede the planning efforts of managers and decision-makers in achieving balance and system stability (EL-Gafy et al., 2017). Consequently, a thorough examination of strategies for mitigating vulnerability requires identifying comprehensive processes and adopting an integrated approach that considers the interrelationships between systems and sectors (Al-Saidi & Elagib, 2017; Ahani et al., 2024). A comprehensive understanding of the system, coupled with a precise evaluation of the

strategies' efficacy in mitigating vulnerability, empowers managers to make informed decisions that enhance adaptability to this phenomenon.

The employment of a nexus approach is instrumental in facilitating the comprehension of systems and their processes, thereby enhancing the efficacy of analysis and problem-solving (Han et al., 2024). The theoretical framework of this approach is systemic and feedback-oriented, enabling the integrated examination of interrelationships among hydrological, economic, and environmental sub-sectors (Keating et al., 2010; Lu et al., 2021). In this context, the employment of a nexus approach constitutes a pivotal strategy for achieving sustainable balance in resource production and consumption. This necessitates the implementation of models that not only meet the essential needs of the current generation but also ensure that future generations can benefit from these resources (Al-Saidi & Elagib, 2017; Ahani et al., 2024).

Among the studies that have employed the nexus approach to examine the impacts of climate change on water resources are those by Lalawmpuii and Rai (2023) and Li et al. (2017). In the present studies, economic, social, and hydrological sectors, as well as the interactions between them, were developed based on the objectives and conditions of the region (Esteve et al., 2015). Analyzing climatic stresses enables the identification of critical areas within the system where adaptation strategies are essential, allowing for the proposal of numerous adaptation measures (Han et al., 2024).

In this study, two effective and targeted approaches were evaluated as strategies to reduce the system's vulnerability to climate change. The two aforementioned strategies are as follows: first, the implementation of an optimal crop pattern policy, and second, the improvement of irrigation efficiency.

Given the critical importance of water as an input in economic activities, changes in its availability due to climate change significantly impact the performance of economic sectors. The interconnected nature of economic, social, and environmental sectors implies that changes in one sector can have ramifications for the others. Consequently, the implementation of these policies under various climate scenarios can offer a clear perspective on future vulnerability. By proposing and examining policies across various dimensions, the effectiveness of adaptation strategies in improving system performance and reducing vulnerability can be evaluated (Chen & Chen, 2016; Li et al., 2017).

Accordingly, this study proposes an integrated model based on the nexus approach, which incorporates the relationships and interactions among hydrological, economic, and environmental sectors to comprehensively assess the impacts of climate change.

The aim of this study is to propose a novel Hydro-Economic-Environmental modeling approach to present adaptation strategies for water resources management in arid and semi-arid regions. This research is based on five main hypotheses: (1) climate change will reduce crop yields and increase water requirements in the Kashfarud River basin; (2) climate change will reduce the water resources available to the agricultural sector in this basin; (3) climate change will lead to a decrease in the optimal area of agricultural land in the aforementioned basin; (4) climate change adaptation policies can reduce greenhouse gas emissions; and (5) these policies

will lead to an increase in farmers' income within the framework of optimal resource allocation. The theoretical foundations of this study require the development of an integrated and multi-sectoral framework in the dimensions of hydrology, economics, and environment.

2 Background

Despite the growing body of research on the Water-Energy-Food (WEF) nexus and hydro-economic modeling, a systematic literature review reveals four fundamental gaps that this study aims to address. First, although multi-objective optimization frameworks have been increasingly applied (Li et al., 2019; Yue & Guo, 2021), very few studies simultaneously integrate blue and green water footprints, carbon footprint, and caloric output as competing objectives within a single nonlinear programming model, particularly for arid regions facing severe water scarcity. Second, most existing integrated models lack rigorous validation protocols, such as hydrological calibration (e.g., using the Nash–Sutcliffe Efficiency coefficient) and systematic sensitivity analyses of critical parameters like water availability and crop prices, thereby limiting their reproducibility and generalizability (Wu et al., 2022; Lodge et al., 2023). Third, while many studies claim scalability to other arid regions, they rarely provide a structured transferability framework that explicitly accounts for institutional, governance, and infrastructural heterogeneity (Esteve et al., 2015; Ahani et al., 2024). Fourth, most climate adaptation studies in Iran have focused on low- or intermediate-emission scenarios (SSP1 and SSP2), whereas recent evidence suggests that current global emission trajectories increasingly align with the high-emission SSP5 pathway, which remains critically understudied in the Iranian context (Mohamad Arbai & Irie, 2025).

Recent methodological advances have increasingly emphasized integrated, multi-objective frameworks for managing interconnected resource systems under climate uncertainty. For instance, multi-objective optimization has been successfully applied to balance economic costs and environmental externalities in complex infrastructure systems, demonstrating how Pareto-front analysis and sensitivity testing can guide robust environmental decision-making (Puchongkawarin, 2024). In parallel, technology-driven nexus approaches have been developed to enhance agricultural resilience in arid and water-scarce regions, highlighting the necessity of precision resource management aligned with sustainable food-energy-water policies (Karanisa et al., 2022). Furthermore, stochastic programming frameworks have been employed to explicitly address climate risk in agricultural investment decisions, revealing how long-term profitability and crop yields are highly sensitive to the probability distributions assigned to future climate trajectories (Jones & Leibowicz, 2022) . Collectively, these studies underscore the growing recognition that isolated sectoral assessments are insufficient for addressing systemic vulnerabilities.

Building on the foundational work of Ahani et al. (2024), this study introduces three key methodological and analytical innovations. First, it develops a novel integrated WEF framework that explicitly captures two-way feedback loops among hydrological, economic, and environmental subsystems within an arid basin. Second, it evaluates the individual and synergistic effects of two Nexus-aligned adaptation strategies—cropping pattern optimization and a 10% improvement in irrigation efficiency—under a range of CMIP6 climate scenarios.

Third, it operationalizes these components within a rigorously validated nonlinear multi-objective optimization model, calibrated and tested against real-world data from the Kashafrud Basin. Collectively, these advances not only bridge the identified methodological gaps but also yield a transferable decision-support framework that can be adapted to other arid basins with comparable hydrological and institutional characteristics.

Accordingly, the study addresses two core research questions: (Q1) How do WEF interdependencies drive climate-induced water resource depletion and exacerbate carbon emissions through increased energy demand for water extraction? (Q2) How do Nexus-aligned adaptive policies, when integrated into an optimal resource allocation framework, influence economic performance and environmental sustainability under future climate conditions?

3 Materials and Methods

The modeling of the Water-Energy-Food Nexus (WEFN) under the influence of changing climatic conditions in the Kashafrud Basin encompasses three study components: climate change, hydrology, environmental, and economic aspects. To that end, a comprehensive analysis of water resources and environmental indicators was conducted. The aforementioned components comprise five phases, as illustrated in Figure 1. The subsequent paragraphs provide a more thorough elaboration on this subject.

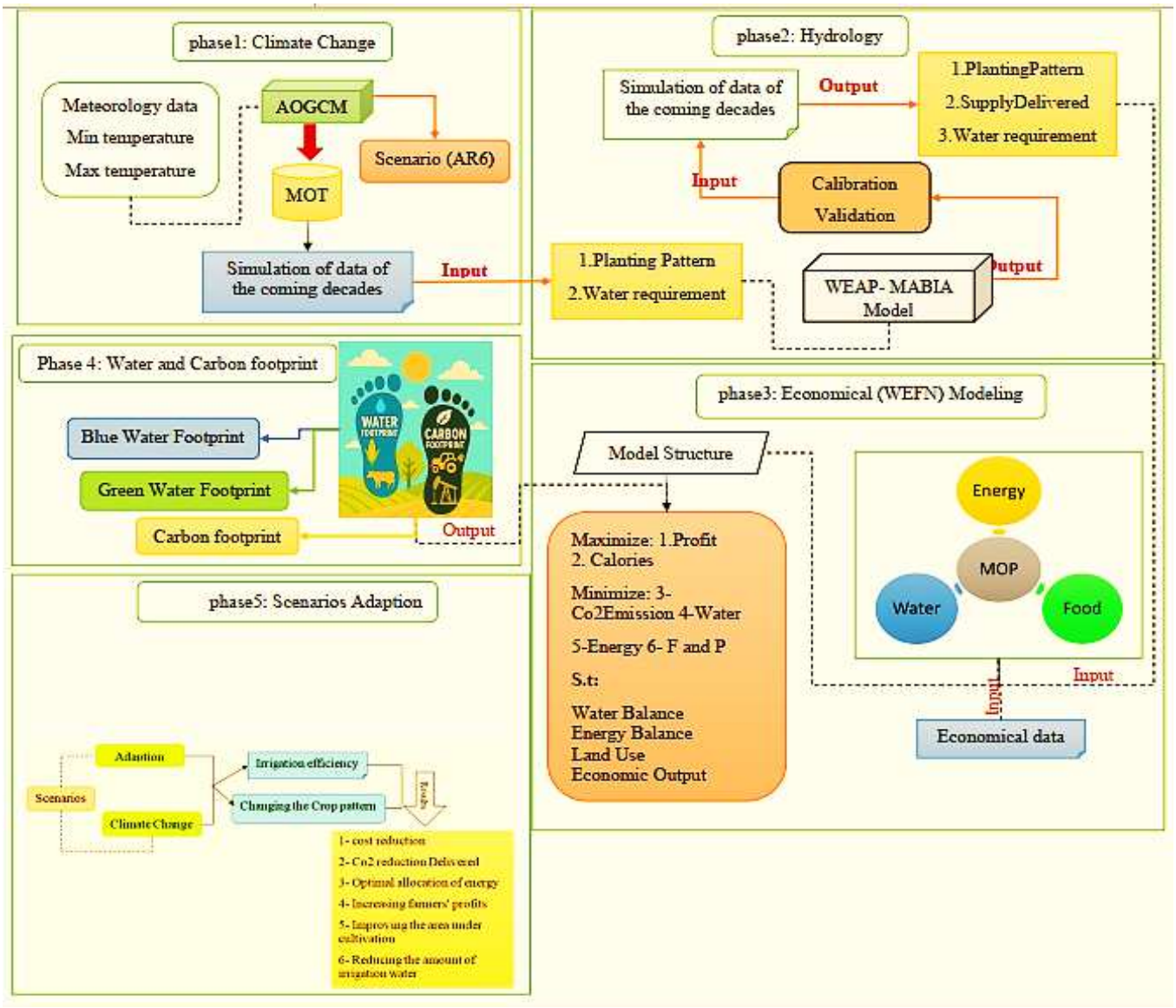


Figure 1. The theoretical structure of the hydrology-economics-environment model

The Hydrology-Economics-Environment Model (HEEM), was simulated for the watershed across five primary phases, as delineated below. The ensuing sections provide detailed explanations for each phase.

3.1 Phase 1: Climate Change

The Intergovernmental Panel on Climate Change (IPCC) periodically issues reports on the state adaptation to this phenomenon, and vulnerability reduction at global and regional scales. The scenarios delineated in the Sixth Assessment Report encompass five primary subgroups, with a pronounced emphasis on quantitative indicators such as population, urbanization, economic development (both regional and transregional), and Shared Socioeconomic Pathways (SSPs) (impacts, adaptation, and vulnerability reduction). Additionally, the report explores energy planning and land-use changes. This phase integrated greenhouse gas forcings and socioeconomic pathways for scenario development. Consequently, this study examined future

changes in temperature and precipitation over the Kashafrud Basin based on the outputs of Phase 6 models.

A weighted combination of four AOGCMs sourced from CMIP6 was utilized to define climatic variability and change, incorporating assumed metrics. The SSP1 (optimistic), SSP3 (pessimistic), and SSP5 (very pessimistic) scenarios were used to predict the baseline (1993–2012) and future (2021–2040) intervals.

Climate change was conducted in two stages. In the first stage, the existing models in the relevant project that had historical temperature and precipitation data as well as the desired scenarios were initially identified. Subsequently, to evaluate the accuracy of these models for the study area, the historical temperature and precipitation data of these models were prepared for the 20-year baseline period of 1993-2012. Finally, for the calibration and validation of the models, the correlation coefficient (r), mean absolute deviation (MAD), root mean square error (RMSE), mean absolute percentage error (MAPE), and Nash-Sutcliffe efficiency coefficient (NSE) statistics were used for a comparative analysis of the models. In these relationships, A_t represents the value of the observational data (monthly observational mean), F_t represents the value predicted by the model (model's historical monthly mean), the subscript t represents the months of the year, and n represents the number of months. The mentioned statistics were calculated using Equations 1 through 4, respectively.

$$\mathrm{MAD} = \frac{\sum_{t=1}^{n} \vdots A_t - F_t \vdots}{n} \quad (1)$$

$$\mathrm{RMSE} = \sqrt{\frac{\sum_{t=1}^{n} (A_t - F_t)^2}{n}} \quad (2)$$

$$\mathrm{MAPE} = \frac{\sum_{t=1}^{n} \frac{A_t - F_t}{A_t}}{n} \times 100 \quad (3)$$

$$\mathrm{NSE} = 1 - \frac{\sum_{t=1}^{n} (A_t - F_t)^2}{\sum_{t=1}^{n} (A_t - A^{\mathrm{mean}})^2} \quad (4)$$

3.2 Phase 2: Hydrology model

A hydrological simulation of the basin was conducted using the Water Evaluation and Planning (WEAP) model and water resource management models. The WEAP model is a water resource planning instrument grounded in the tenet of water balance, which delineates various sub-basins, water demand nodes, infrastructure, water flows, and transmission channels. Consequently, each sub-basin unit is segmented into discrete land-use classes, and the water balance for that sub-basin is calculated under its specific climatic conditions. The workflow of this module is comprised of two stages, which are delineated as follows.

- *Calculation of Crop Evapotranspiration*

Calculating the available water capacity is a critical step in this process. Available water capacity was calculated using data related to the soil's water-holding capacity at saturation. The calculation took into account the region's soil texture type, field capacity, and the plant's wilting point.

- *Estimation of Irrigation Water Requirements*

The regional water demand for irrigation in agriculture for crops in each region were modeled through the implementation of irrigation scheduling and the determination of irrigation depth. The MABIA module was utilized to simulate hydrological processes. In essence, the utilization of diverse agricultural, hydrological, and meteorological data facilitated the simulation of crop yield and water requirements.

This is based on the MABIA computational method. Crop latent heat flux is calculated using the FAO 56 model (Allen et al., 2005). Evapotranspiration calculations require meteorological data such as temperature, minimum and maximum temperature, wind velocity at two meters, and hours of sunshine (White et al., 2018). The MABIA module uses equation 5 to simulate crop yield. In this equation, $Y_a$is the actual crop yield; Y_m, the maximum yield; K_y , the yield response factor; and ET_a, the actual evapotranspiration. ET_c is the evapotranspiration under natural conditions without limitations.

$$1 - \frac{Y_a}{Y_m} = K_y \left(1 - \frac{ET_a}{ET_c}\right) \quad (5)$$

3.3 Phase 3: Mathematical Programming Framework for SWEFN

Utilizing the findings from Phases One and Two, the Sustainable Integrated Nexus for Water, Energy, and Food Security were examined, and the allocation of inputs under various climate pathways. The impact of adaptation policies under climate change conditions across hydrological, economic, and environmental dimensions was modeled using mathematical programming methods. These methods were based on study by Peng et al. (2022).

The core of the Sustainable Water–Energy–Food Nexus (SWEFN) model is a multi-objective programming (MOP) framework to evaluate farmers' adaptation to changing climatic conditions. This model has the capacity to process management decisions based on a variety of objectives. The model's framework encompasses not only economic considerations but also the control of greenhouse gas emissions and environmental impacts. Therefore, six objectives were incorporated into the current study to ensure model flexibility, enabling the evaluation of different goals across various dimensions as outlined below.

The present study is guided by the following objectives:

i. Maximization of gross profit;
ii. Maximization of caloric output from food production systems;
iii. Reduction in the application of synthetic fertilizers and pesticides; and
iv. Minimization of resource and environmental burdens, specifically irrigation water consumption, energy use, and greenhouse gas (GHG) emissions.

The complete mathematical formulation of the multi-objective programming (MOP) model including all six objective functions and the full set of system constraints (e.g., water and energy balances, land and production limits, and food security thresholds). Constraints ensure physical and institutional feasibility by governing resource availability, infrastructure capacity, and minimum production requirements, while maintaining non-negativity of decision variables.

The corresponding objective functions are formally defined in Equations (6) through (11).It is noteworthy that the decision variables in this study are designated with the letter "v," while the observational data are denoted with the letter "p."

Max: Obj1Profit_V

$$= \sum_{i=1}^{I}\left[\left(\text{Price_P}_{k} \,.\, \sum_{k=1}^{K} \text{Yield_P}_{ik} \,.\, \text{CultArea__V}_{ik}\right)\right.$$
$$- \left(\text{Watcos_P}_{ik}.\left(\sum_{k=1}^{K} \frac{\text{SurWat_}V_{ik}}{\text{SurwatCoe_P}_{i}}\right) + \text{GroWatCos_P}_{ik}.\left(\sum_{k=1}^{K} \frac{\text{GrowatNet_}V_{ik}}{\text{GrowatCoe_P}_{i}}\right)\right.$$
$$+ \left(\text{TranCos_P}_{i}\left(\sum_{k=1}^{K} \text{Esurwat_}V_{ik} + \text{EGrouwate_}V_{ik}\right)\right.$$
$$+ \text{EProcCos_P}_{i}\left(\sum_{k=1}^{K} \text{ElectFood_}V_{i}\right) + \sum_{k=1}^{K} \text{FertCos_P}_{ik} + \text{PestCos_P}_{ik}$$
$$\left.\left.\left.+ \text{OpeAgriCos_P}_{ik}\right) + (\text{Cost_P}_{ik} + \text{FilmCos_P}_{k}).\left(\sum_{k=1}^{K} \text{CultArea__V}_{ik}\right)\right)\right] \quad (6)$$

The components of the objective functions are defined as follows:

Obj1Profit_V: Maximization of farmers' gross profit (Iranian Rial (IRR) ha^{-1}), expressed as the difference between total revenue and total production costs.

Price_P_{k}: Market price of agricultural output k (IRR kg^{-1}).

Yield_P_{ik}: Crop yield of product k in region i (ton ha^{-1}).

CultArea__V_{ik}: Cultivated area allocated to crop k in region i (ha).

279 $\mathrm{Watcos_P_{ik}}$: Operational cost of surface water use for irrigating crop *k* in region *i* (IRR ha^{-1}).

280 $\mathrm{SurWat_}V_{ik}$: Net volume of surface water allocated to crop *k* in region *i* for food production
281 (m^3).

282 $\mathrm{SurwatCoe_P_i}$: Surface water utilization coefficient for crop *i* (dimensionless).

283 $\mathrm{GroWatCos\ _P_{ik}}$: Operational cost of groundwater extraction for crop *k* in region *i* (IRR ha^{-1}).

284 $\mathrm{GrowatNet\ _}V_{ik}$: Net volume of groundwater assigned to crop *k* in region *i* (m^3).

285 $\mathrm{GrowatCoe_P_i}$: Groundwater utilization coefficient for crop *i* (dimensionless).

286 $\mathrm{TranCos\ _P_i}$: Cost of electricity consumed for water transmission and distribution in region *i*
287 (IRR ha^{-1}).

288 $\mathrm{Esurwat_}V_{ik}$: Electricity quota allocated for pumping surface water for crop *k* in region *i*
289 (kWh).

290 $\mathrm{EGrouwate_}V_{ik}$: Electrical energy allocated for groundwater pumping for crop *k* in region *i*
291 (kWh).

292 $\mathrm{EProcCos_P_i}$: Regional cost of electricity in the agri-food sector (IRR ha^{-1}).

293 $\mathrm{ElectFood_}V_i$: Total energy throughput allocated to regional food systems (kWh).

294 $\mathrm{FertCos_P_{ik}}$: Fertilizer input cost for crop *k* in region *i* (IRR ha^{-1}).

295 $\mathrm{PestCos\ _P_{ik}}$: Pesticide input cost for crop *k* in region *i* (IRR ha^{-1}).

296 $\mathrm{OpeAgriCos\ _P_{ik}}$: Operational cost of agricultural machinery for crop *k* in region *i* (IRR ha^{-1}).

297 $\mathrm{Cost_P_{ik}}$: Aggregate production cost for crop *k* in region *i* (IRR ha^{-1}).

298 $\mathrm{FilmCos\ _P_k}$: Cost of agricultural plastic mulch per hectare for crop *k* (IRR ha^{-1}).

299 The second objective, denoted as $\mathrm{Obj2Coleri_}V$, aims to maximize the total dietary energy
300 (caloric) output derived from cultivated crops (Equations (2)).

$$\mathrm{Max:\ Obj2Coleri_}V = \sum_{i=1}^{I}\left(\mathrm{Enp_P_k}.\mathrm{Yield_P_{ik}}\sum_{k=1}^{K}\mathrm{CultArea__V_{ik}}\right) \quad 7$$

301 Where, $\mathrm{Enp_P_k}$ represents the energy content (kcal) per unit mass of crop *k*.

302 The third objective, $\mathrm{Obj3FP_}V$, seeks to minimize the total application of synthetic fertilizers
303 and pesticides across all crops and regions:

$$\mathrm{Min:\ Obj3FP_}V = \sum_{i=1}^{I}\sum_{k=1}^{K}(\mathrm{FertiCon\ _P_{ik}} + \mathrm{pesticide_P_{ik}}).\mathrm{CultArea__V_{ik}} \quad 8$$

Where:

FertiCon _P_{ik}: is the fertilizer application rate for crop k in region i (kg ha^{-1});

pesticide_P_{ik}: is the pesticide application rate for crop k in region i (kg ha^{-1});

The fourth objective (Equation 4), denoted as Obj4Wat_V, minimizes total irrigation water consumption by normalizing actual water allocations against regional agricultural water availability ratios:

$$\text{Min: Obj4Wat_}V = \sum_{i=1}^{I}\sum_{k=1}^{K}\left((\text{SurWat_}V_{ik}/\text{Surwater_P}_i) + (\text{GrowatNet }_V_{ik}/\text{Growater_P}_i)\right) \quad (9)$$

Surwater_P_i and Growater_P_i are agricultural surface and groundwater utilization ratio for each region, respectively.

The fifth objective, Obj5Energy Elec_V, seeks to minimize total energy use associated with water management and food system operations (Equation 5).

$$\text{Min Obj5Energy Elec_}V = \sum_{i=1}^{I}\sum_{k=1}^{K}(\text{AE Resou_V}_i + \text{ElectFood_V}_i) \quad (10)$$

where:

AE Resou_V_i: denotes the energy consumed for water extraction, conveyance, and distribution in region i (kWh);

ElectFood_V_i: represents the electrical energy allocated to regional food processing and post-harvest activities (kWh).

As shown in Equation (6), the sixth objective—denoted as Obj6CO2_V —aims to minimize total greenhouse gas (GHG) emissions associated with agricultural production. The emission inventory encompasses the following components:

$$\begin{aligned}\text{Min: Obj6CO2_}V &= \sum_{i=1}^{I}\sum_{k=1}^{K}\big((\text{DieselCo2_P.DieselCon_P}_i + \text{FilmCo2_P.FilmCon }_P_i \\ &+ \text{PestiCo2_P.pesticide_P}_{ik} + \text{ElecCo2_P.ElecCon }_P_{ik} + \text{FoodCo2 }_P\text{ .ElectFood_V}_i \\ &+ \text{Ferti}Co2\text{_P.FertiCon }_P_{ik}\text{).CultArea__V}_{ik}\big)\end{aligned} \quad (11)$$

The emission inventory encompasses the following components:

- Diesel combustion: represented by the carbon emission coefficient of diesel fuel (DieselCo2_P, kg CO_2 L^{-1}) and diesel consumption (DieselCon_P_i,i , L ha^{-1});

- Agricultural plastic mulch: characterized by its emission coefficient ($\mathrm{FilmCo2_P}$, kg CO_2 kg^{-1}) and application rate ($\mathrm{FilmCon_P_i}$,i , kg ha^{-1});
- Pesticide use: quantified via the emission factor ($\mathrm{PestiCo2_P}$, kg CO_2 kg^{-1} active ingredient) and pesticide application rate ($\mathrm{pesticide_P_{ik}}$, kg ha^{-1});
- Electricity for irrigation: modeled using the grid emission factor ($\mathrm{ElecCo2_P}$, kg CO_2 kWh^{-1}) and crop-specific electricity consumption ($\mathrm{ElecCon\ _P_{ik}}$, kWh ha^{-1});
- Electricity for food processing: accounted for through the emission coefficient for processing energy ($\mathrm{FoodCo2\ _P}$, kg CO_2 kWh^{-1}) and the allocated energy throughput (ElectFood_V_i, kWh);
- Fertilizer application: captured by the emission coefficient of synthetic fertilizers ($\mathrm{Ferti}Co2_\mathrm{P}$, kg CO_2 kg^{-1} N or compound) and the applied fertilizer rate ($\mathrm{FertiCon\ _P_{ik}}$, kg ha^{-1}).

Given the plurality of conflicting objectives outlined above, this study adopts a multi-objective programming (MOP) approach to address the trade-offs among them. The solution methodology—specifically, the framework for handling multiple nonlinear objectives—was adapted from the approaches proposed by Fabiani et al. (2020), Li et al. (2019), and Mardani Najafabadi et al. (2019), rather than replicating their optimization models. This allows for a context-sensitive application of established multi-objective resolution techniques to the present agricultural sustainability problem.

Constraints

The following sections detail the constraints of the objective function.

1. Electricity Consumption Constraints

The electricity consumed for pumping and distributing surface and groundwater must not exceed the region-specific energy limit. This is formalized in Equation (12):

$$\mathrm{SurWatPum\ _P_i}\left[\left(\frac{\sum_{k=1}^{k}\mathrm{SurWat_}V_{ik}}{\mathrm{Surwater_P_i}}\right)+\mathrm{EGrouWate_P_i}\left[\left(\frac{\sum_{k=1}^{k}\mathrm{GrowatNet\ _}V_{ik}}{\mathrm{Growater_P_i}}\right)\right]\right]\leq \mathrm{AE\ Resou_V_i} \qquad 12$$

Here, ($\mathrm{SurWatPum\ _P_i}$, kWh m^{-3}) denotes the energy required to pump one cubic meter of surface water, and ($\mathrm{EGrouWate_P_i}$, kWh m^{-3}) represents the energy intensity of groundwater extraction in region i. These parameters serve as key indicators of energy efficiency in the water sector.

2. Constraints on Energy Consumption in Food Production and Processing

Total electricity consumption across the food value chain must remain within the regionally allocated energy budget for agriculture (Equation 13):

$$\sum_{k=1}^{k} (\text{EleFoodProd_P}_{ik} \,.\, \text{Yield_P}_{ik}).\, \text{CultArea_V}_{ik} \leq \text{ElectFood_}V_i \quad \forall_i \qquad 13$$

The parameter ($\text{EleFoodProd_P}_{ik}$, kWh kg^{-1}) reflects the electricity intensity of producing one kilogram of crop *k* in region *i*.

3. Constraints on Available Energy for Water Transfer

The combined energy demand for water supply and food production cannot exceed the net energy available for agriculture after subtracting non-agricultural consumption (Equation 14):

$$\text{AE Resou_V}_i + \text{ElectFood_V}_i \leq \text{AvaEnergy _P}_i - \text{EnergyCon_P}_i \qquad \forall_i \qquad 14$$

In equation 9:

where (AvaEnergy _P_i, kwh) is the total energy supply in region, and (EnergyCon_P_i, kwh) represents energy used by industrial and residential sectors.

4. Constraints on Surface Water Allocation

The total surface water allocated to crops cannot exceed the available supply from infrastructure (Equation 15):

$$\frac{\sum_{k=1}^{k} \text{SurWat_V}_{ik}}{\text{Surwater_P}_i} \leq \text{WatSupply_P}_i \,.\, \text{Surwater_P}_i \quad \forall_i \qquad 15$$

Here, (WatSupply_P_i, m^{-3}) denotes the total surface water delivered via municipal and irrigation systems.

5. Constraints on Groundwater Allocation

Similarly, groundwater abstraction must respect pumping capacity limits (Equation 16):

$$\frac{\sum_{k=1}^{k} \text{GrowatNet _V}_{ik}}{\text{Growater_P}_i} \leq \text{Gw_P}_i.\, \text{Growater_P}_i \;\; \forall_i \qquad 16$$

The parameter (Gw_P_i, m^3) represents the maximum allowable groundwater extraction volume in region *i*.

6. Constraints on Water Allocation

For each crop k in region i , the sum of surface water, groundwater, and effective rainfall must meet the crop's water requirement (Equation 17):

$$\mathrm{SurWat_V_{ik}} + \mathrm{GrowatNet_V_{ik}} + (\mathrm{Ep_P_{ik}}.\mathrm{CultArea_V_{ik}}) \geq \mathrm{WatReq_P_{ik}}.\mathrm{CultArea_V_{ik}} \quad \forall_i \tag{17}$$

where $(\mathrm{Ep_P_{ik}}, \mathrm{m^3 ha^{-1}})$ is effective rainfall, and $(\mathrm{WatReq_P_{ik}}, \mathrm{m^3 ha^{-1}})$ is the crop water requirement.

7. Constraints on Maximum and Minimum Cultivable Land Area

Cultivated area for each crop is bounded by agronomic and policy-driven thresholds (Equation 18):

$$\mathrm{La_P_{ik}^{min}} \leq \mathrm{CultArea_V_{ik}} \leq \mathrm{La_P_{ik}^{max}}, \qquad \forall_i, k \tag{18}$$

8. Constraints on Maximum and Minimum Agricultural Production

Total production of each crop must satisfy minimum food security requirements and not exceed market or storage limits (Equations 19–20):

$$\sum_{i=1}^{I} \mathrm{CultArea_V_{ik}}.\mathrm{Yield_P_{ik}} \leq \mathrm{Dem_P_{ik}^{Max}}, \qquad \forall_k, i \tag{19}$$

$$\sum_{i=1}^{I} \mathrm{CultArea_V_{ik}}.\mathrm{Yield_P_{ik}} \geq \mathrm{Dem_P_{ik}^{Min}}, \qquad \forall_k, i \tag{20}$$

The lower bound ($\mathrm{Dem_P_{ik}^{Max}}$ *and* $\mathrm{Dem_P_{ik}^{Min}}$ limits) ensures baseline food availability, thereby integrating food security into the optimization framework alongside economic and energy objectives.

9. Non-negativity

The ninth constraint: The non-negativity condition for the model variables is finally defined by Equation 21.

$$
\begin{aligned}
&\text{SurWat_V}_{ik} \geq 0 && , && \forall_i, k \\
&\text{SurWat_V}_{ik} \geq 0 && , && \forall_i, k \\
&\text{GrowatNet _V}_{ik} \geq 0 && , && \forall_i, k \\
&\text{CultArea__V}_{ik} \geq 0 && , && \forall_i, k \\
&\text{SurWatPum _V}_{ik} \geq 0 && , && \forall_i, k \\
&\text{EGrouWate_V}_{ik} \geq 0 && , && \forall_i, k \\
&\text{EleFoodProd_V}_{ik} \geq 0 && , && \forall_i, k \\
&\text{AE Resou_V}_{i} \geq 0 && , && \forall_i, k \\
&\text{ElectFood_}V_i \geq 0 && , && \forall_i, k
\end{aligned}
\qquad 21
$$

3.4 Phase Four: Water and Carbon Footprint

The components of water and energy footprints were calculated using the results from Phases 1 to 3. This calculation was performed to ensure proper management of resource and input consumption, as well as to optimize water usage and greenhouse gas emissions. Consequently, a crop pattern that is well-suited to the regional conditions was selected. The green and blue water footprints for crops in the studied basin of Khorasan Razavi Province were computed based on methodologies from Cheng et al. (2011) and Ababaei et al. (2014).

The volume of blue water consumption $\text{CWU}_{\text{blue,Irr}}$ and green water consumption $\text{CWU}_{\text{green,Irr}}$was estimated based on Equation 22, respectively.

$$\text{WF}_{\text{Blue,Irr_V}_i} = \text{NetIrrReq} = 10 * \text{IE} * \text{GroIrrr} \qquad 22$$

It is worth mentioning that the green and blue water footprints, expressed in cubic meters per ton, are also calculated from the ratio of green and blue water consumption to the quantity of produced yield in m3/ton of product, based on Equations 23 and 24.

$$\text{WF}_{(\text{Crop,Blue})_}\text{V}_{ik} = \frac{\text{WF}_{\text{Blue,Irr_P}_{ik}}}{\text{Y_P}_{ik}} \qquad 23$$

$$\text{WF}_{(\text{Crop,Green})_}\text{V}_{ik} = \frac{\text{WF}_{\text{Green,Irr_P}_{ik}}}{\text{Y_P}_{ik}} \qquad 24$$

The carbon footprint in this study was calculated using the method from (Cheng et al., 2011). It is the sum of carbon dioxide emissions resulting from the consumption of fossil fuels, fertilizers, pesticides, electricity, plastic mulch rolls, and irrigation water per cultivated area of each crop. This is achieved by multiplying the consumption of each agricultural input by its respective carbon content coefficient and dividing by the crop yield, as per Equation 25

(Mohammadi et al., 2024). Accordingly, the variable $CE_{Co2}_V_{ik}$ represents the carbon footprint of the crops.

$$CE_{Co2V_{ik}} = \sum_{i=1}^{I} \frac{\begin{pmatrix} Ferti Co2_P . FertiCon \sum_{k=1}^{k} Area_{P_{ik}} + PestiCo2_p . pesticide_{Pik} . \sum_{k=1}^{k} Area_{P_{ik}} + \\ FilmCo2_P . FilmCon_{P_{ik}} + \sum_{k=1}^{k} Area_{P_{ik}} + Ced . DieselCon \sum_{k=1}^{k} Area_{P_{ik}} + \\ ElecCo2 . Eia . \theta_i \sum_{k=1}^{k} Area_{P_{ik}} \end{pmatrix}}{\sum_{k=1}^{k} Yield_{P_{ik}}} \quad (25)$$

3.5 Phase Five: Adaptation Scenarios

A range of scenarios has been devised to optimize resource management under the water-energy-food nexus approach. The objective is to enable farmers to formulate climate adaptation strategies. The first scenario examined in this study is the baseline scenario, against which all subsequent changes are compared and evaluated. The second scenario involves altering crop patterns. Essentially, this scenario involves modifying the cultivated area to address the effects of climate change. The irrigation efficiency improvement scenario is promising for further research. In this scenario, improving irrigation efficiency by 10% mitigates the adverse impacts of climate change on the agricultural sector compared to baseline climate change conditions. Finally, integrating policies and assumptions from previously defined scenarios enables a comprehensive evaluation through combined scenarios. For a more thorough examination of this phase, please refer to Table 1.

Table 1. Climate Change Adaptation Policies

Scenario	Description
Reference Scenario	This scenario represents the current state of affairs (business as usual). It serves as a baseline for other scenarios involving specific policy interventions. In essence, the baseline scenario only examines water consumption, crop yields, unmet and meetable water demand up to the time horizon of the scenarios, assuming no new water resource development projects are implemented and no climate change impacts are considered.
Crop Pattern Change	Water scarcity increases the opportunity cost of water. Farmers adapt by shifting their cultivation patterns towards crops with higher marginal value of production and reducing or eliminating the cultivation of crops with lower value. This strategy aims to mitigate the economic losses from climate change compared to a situation where farmers continue their existing cultivation patterns without regard to water shortages. In other words, this scenario involves adjusting the cultivated area as the key variable to achieve adaptation to climate change effects, as realized in Scenario 3.

Irrigation Efficiency Improvement	In this scenario, a 10% increase in irrigation efficiency can help mitigate the negative impacts of climate change on the agricultural sector. Government agencies in these regions aim to achieve this increase through a five-year program that includes extension services, improving farmers' knowledge, and introducing more modern equipment. Therefore, the effects of this policy need to be evaluated. Generally, this scenario assumes that while the cultivated area remains constant, irrigation efficiency in agricultural lands increases by 10% through the adoption of modern irrigation methods such as drip and sprinkler irrigation, lining water conveyance canals, land leveling in surface-irrigated areas, and other similar measures.
Combined Scenarios	This series of scenarios combines the policies and assumptions defined in the previous individual scenarios. In other words, under these combined scenarios, the various measures and conditions from the earlier scenarios are assumed to be present simultaneously in the Mashhad study area's water resources and consumption. Their combined effects are evaluated together.

3.6 Validation and Sensitivity Analysis

To ensure the reliability and predictive capacity of the integrated hydro-agricultural modeling framework, a systematic calibration and validation protocol was implemented, complemented by a formal sensitivity analysis to quantify parameter uncertainty and model robustness. Model calibration and validation were conducted by comparing simulated outputs against observed field data for key agronomic and hydrological variables, specifically crop yield and net irrigation water requirements. The Parameter ESTimation (PEST) tool—a model-independent, gradient-based optimization algorithm—was employed to automate parameter adjustment and minimize the objective function between simulated and observed values within the WEAP modeling environment. PEST iteratively adjusts sensitive parameters (e.g., crop coefficients, soil water retention parameters, irrigation efficiency factors) to maximize goodness-of-fit metrics while avoiding overfitting through regularization constraints. The calibration period spanned the hydrological years 2014–2015, while validation was performed using independent data from 2015–2019.

3.7 Data Sources and Software

This study gathered data from a wide range of reliable sources, including regional water companies, agricultural and planning organizations, natural resources and meteorology departments, as well as consulting firms and key reference materials. The statistical and performance reports further corroborated the quantitative and qualitative analyses. This diversity of sources enabled a comprehensive, multidimensional examination of water resources, agriculture, and climate in Khorasan Razavi Province, ensuring accurate, data-driven results with significant scientific and practical value. The calibrated model was executed under all prospective climate scenarios. The resulting data on crop yield, water consumption, and economic profit are openly available (Ahani et al., 2023).

3.8 Solution Algorithm and Software Implementation

The development of the Water-Energy-Food Nexus (WEFN) optimization management model across multiple economic and environmental sectors, has been conducted using

mathematical programming methods and the GAMS software. The model has the capacity to simulate interactions and interdependencies among the three systems. The selected optimization method to solve this model is CONOPT4, a powerful tool for solving large-scale nonlinear programming problems.

3.9 Evaluating the Model's Applicability in the Real World

As previously outlined, the present study took a pioneering approach, using computational optimization methods to examine the effects of adaptation policies on the nexus of resources in the context of climate change. The model was developed for three critical sectors—hydrology, the environment, and economics—as a hypothetical system under constrained conditions, targeting critical regions such as Iran. Since many of Iran's river basins have hot, arid climates, the model was developed for northeastern Iran. The Kashafrud Basin was chosen as the study area because of its severe water resource constraints.

As illustrated in Figure 2, the basin encompasses an area of 9,908 square kilometers, with approximately 66% situated in highlands and 34% in plains. The most significant river in this area is the Kashafrud River. The average annual inflow at the Olang-Esadi station, located at the outlet of the study area, is 28.8 million m3. Subsequent to traversing a distance of 300 kilometers, the body of water discharges into the Harirod River. A comprehensive evaluation of the available data reveals that this basin exhibits a general paucity of surface water resources. The management of water resources in this basin is predicated on the recognition that the topography is characterized by vast, fertile lands interspersed with densely populated areas. Consequently, a primary objective of water resource management is the harnessing and utilization of the limited surface water resources. The region's surface water resources are comprised of various bodies, including dams, rivers, streams, and canals, which are predominantly sustained by snow-rain regimes.

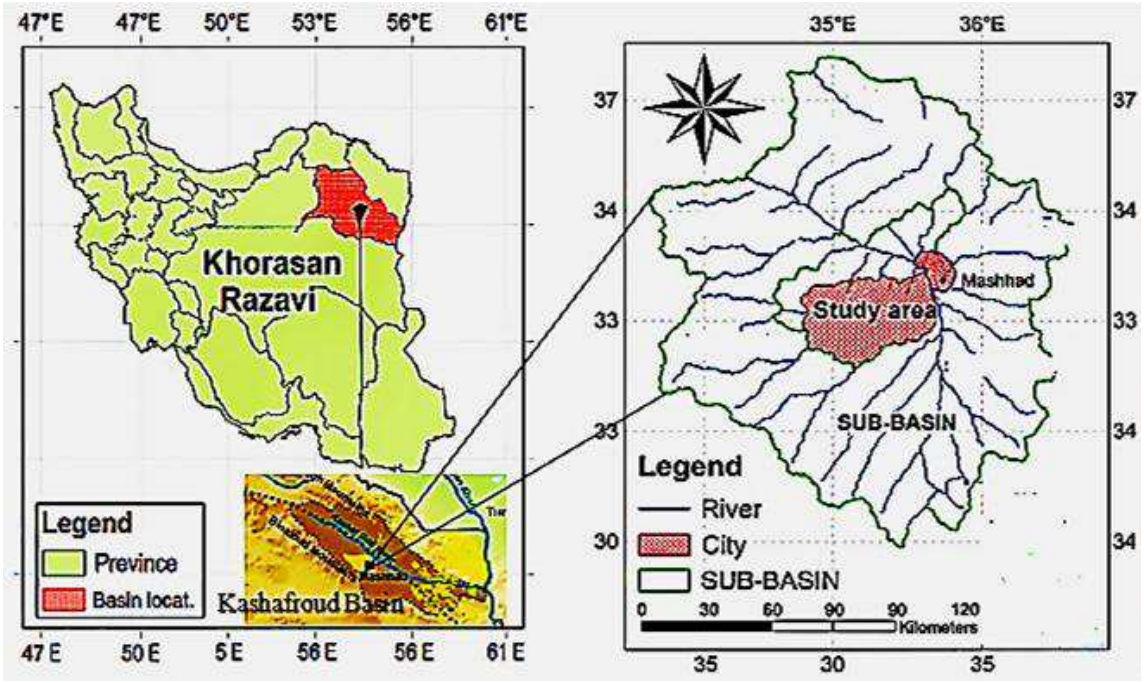


Figure 2. Geographical location and hydro-climatic context of the Kashafrud River Basin.

4 Results

The construction of the hydrological, agricultural, and economic models necessitated a substantial amount of data, encompassing hydrology, crop agriculture, costs, crop yield, soil science, crop irrigation, crop CO2 emission coefficients, electricity consumption, climate, water resources and demands, inflows and outflows from groundwater resources, demand nodes (urban, agricultural, and industrial), and other pertinent factors. The data presented herein were meticulously collected from a variety of public and private sources, as well as from credible reports, and were subsequently disaggregated by crop. At this stage, a list of some of the data required for the MABIA model for crops is provided.

Other required data for the MABIA model include crop coefficients (Kc) and the yield response factor to water (Ky) for agricultural crops, which are provided in Table 2. In addition to this information, field capacity, wilting point, available moisture, soil texture characteristics, irrigation details, moisture depletion from the upper and lower soil layers, effective precipitation, weather data, and other plant physiology information were also input into the model.

Table 2 Crop Coefficients for Agricultural Products

	Ky			**Kc**			
Product	Late	Mid-Season	Development	Initial	Mid-Season	Development	Initial
Wheat	0.40	0.50	0.60	0.2	0.15	1.10	0.15
Barley	0.40	0.48	0.60	0.50	0.15	1.10	0.15
Sugar beet	1	1.2	0.80	0.5	0.70	1.20	0.35
Onion	0.2	0.55	0.40	0.2	0.70	1.05	0.15
Potato	0.10	0.10	0.10	0.10	0.75	1.05	0.50
Tomato	0.80	1.1	0.60	0.5	0.70	1.15	0.60
Alfalfa	0.10	0.10	0.10	0.10	1.10	1.15	0.30
Maize	0.60	0.60	0.60	0.60	1	1.10	0.14
Cucumber	0.10	0.10	0.10	0.10	0.75	1	0.60

In order to construct a model of the water-food-energy nexus in the Kashafrud River Basin, there are several pieces of essential data that must be taken into consideration. These include the cultivated crop area, the quantity of fertilizer and pesticide usage, the crop yields, the net irrigation requirement, the caloric output from crop production, and the electricity consumption (Table 3).

Table 3. List of Basic Information for Cultivated Crops in the Basin

Crop	Electricity (kWh/ha)	Yield (ton/ ha)	Fertilizer (t/ha)	Pesticides (kg/ha)	Area (ha)	Calorie production (kilo)	Gross water requirement (mcm)
Wheat	2969	4.2	392	1.391	22254	3500	6644
Barley	2492	3.6	364	0.962	21261	3890	5577
Sugar beet	9057	35	572	4.38	2385	460	20266
Onion	6842	50	606	4.18	1149	400	1511
Potato	8759	35	706	3.64	323	770	19600
Tomato	8054	40	641	2.97	5869	180	18022
Alfalfa	8272	11	253	0.95	5385	230	18511
Maize	6078	55	543	2.13	4460	860	13600
Cucumber	5859	25	456	4.18	920	120	13111
Total	53382	90992	4533	24.79	64006	10410	116842

4.1 Climate Change

Initially, a meticulous evaluation of climate models was conducted by comparing their historical data on temperature and precipitation with observed data, employing various statistical indicators to ensure accuracy. The findings indicated that the model demonstrated high performance, as evidenced by the model assessment statistics (MAD), root mean square error (RMSE), mean absolute percentage error (MAPE), and Nash-Sutcliffe efficiency (NSE) of 0.96 for precipitation and 0.97 for temperature (Table 4).

The correlation coefficient values across the basin for different models, between simulated and observed data for precipitation and temperature variables, are above 0.70. This indicates a high average correlation coefficient for precipitation and temperature variables, which are 0.98 and 0.99 respectively, generally close to 1. This value was also calculated as 0.98 for all models. Furthermore, across the different models, the Nash-Sutcliffe efficiency (NSE) values are greater than 0.5.

Overall, the Nash-Sutcliffe efficiency coefficient for precipitation and temperature variables is 0.96 and 0.97, respectively, indicating the high performance of the models within the basin. The model validation results demonstrate that the model simulations are highly consistent with the observed data.

Table 4:Model Evaluation in the baseline period (1994-2021) through calibration statistics

Variable	MAD	RMSE	MAPE	NSE	R
Rain	2.38	3.69	11.95	0.96	0.98
temperature	0.95	1.22	8.91	0.97	0.99

Subsequently, a series of future scenarios were examined, with the pessimistic scenario forecasting a negligible increase in precipitation, while the remaining two scenarios indicated no substantial alterations. However, maximum monthly temperatures were projected to increase by approximately 6.95 degrees Celsius during the 2021-2040 period compared to the baseline period (Figure 3). These findings carry significant implications for the implementation of adaptation policies, which could result in substantial alterations in resource management and future decision-making processes.

Precipitation during the spring season increased across all scenarios by 4.28% to 6.95% (Table 5). In contrast, precipitation decreased during the summer and autumn seasons in all scenarios. The lowest values were observed in summer, ranging from -10.67% to -21.81%, and in autumn, ranging from -1.36% to -3.4%. Winter precipitation showed a very slight increase only under the pessimistic scenario, while the other two scenarios did not exhibit significant changes. Regarding temperature, the baseline period average was 18.66°C. Under the optimistic, moderate, and pessimistic scenarios, temperatures are projected to increase by 6.17°C, 6.19°C, and 6.95°C, respectively, by the year 2040 across different months.

Table 5. Seasonal Precipitation Changes during 2021-2040 (mm)

Season	SSP1	SSP3	SSP5	Observed
Winter	142.66	141.24	147.25	142.32
Spring	86.82	86.57	88.79	83.02
Summer	6.74	7.14	7.7	8.62
Autumn	62.63	62.3	63.61	64.49

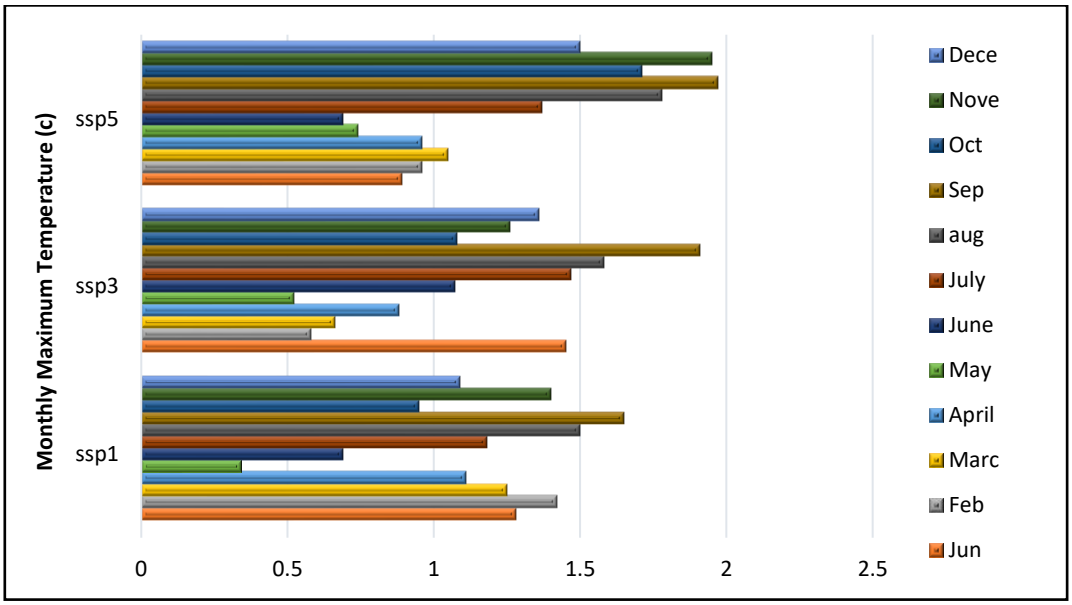
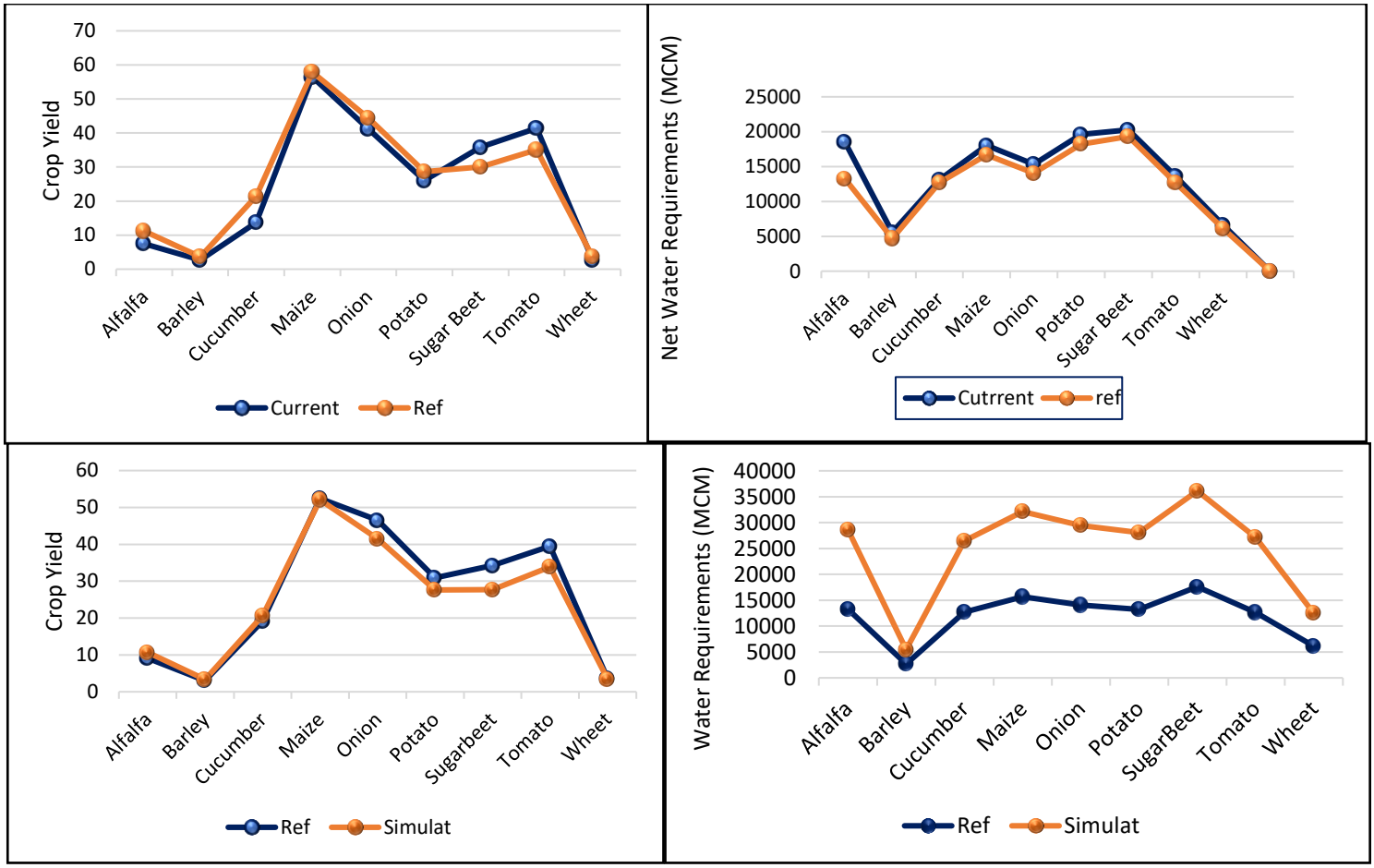


Figure 3. Monthly Maximum Temperature Changes for the Period 2021-2040 Compared to the Baseline Period

4.2 Model Validation and Robustness Assessment

Figure 4 presents the comparative evaluation of simulated versus observed values for two key agronomic indicators—net irrigation water requirements and crop yields—across the agricultural zones of the Kashafrud Basin. The baseline period (2012–2013) was used for model initialization, while the validation period spanned 2013–2021, encompassing both normal and drought hydrological years to test model performance under climatic variability.

Model performance was assessed using a dual-criteria framework: (i) relative error (RE) classification, and (ii) standard hydro-agricultural goodness-of-fit metrics. Following established guidelines, RE thresholds were defined as: excellent ($|RE| < 10\%$), good ($10\% \leq |RE| < 20\%$), satisfactory ($20\% \leq |RE| < 30\%$), and unsatisfactory ($|RE| \geq 30\%$). The basin-aggregated mean relative error across all crops and years was 18.3%, falling within the "good" performance category and indicating that the model reliably reproduces observed hydro-agricultural dynamics at the spatial scale of interest.



576 Figure 4. Verification and validation of water requirement and crop yield parameters

577 4.3 Comparison of Water Requirements and Crop Yields under Climate 578 Change Scenarios

579 A series of simulations were conducted to assess the potential impact of shifting climatic
580 conditions on crop yield and net water requirements within the basin (Table 6). These
581 simulations, conducted up to the year 2040, revealed a decline in average overall crop yield of
582 20 tons, accompanied by a decrease in net water requirement for crops within the basin by
583 17,734 million m3 per ha. The most substantial decline in yield was observed in forage crops.

584 Among the crops examined across the basin, forage corn experienced the largest yield
585 reduction under the pessimistic scenario, with a decrease of 23 tons, while alfalfa had the
586 smallest reduction, with a decrease of 8 tons. Additionally, the net water requirement of the
587 crops was severely impacted under pessimistic conditions due to rising temperatures, with
588 potato and sugar beet having the highest and lowest net water requirements, respectively, under
589 these conditions. Overall, the simulation of net water requirements and crop yields up to the
590 year 2040, using hydrological modeling, has been reported.

591

592 Table 6. Simulation of Crop Yield and Net Water Requirements Under Climate Change
593 Conditions

Variable	crops	ref	SSp1	SSp3	SSp5
Yield	Wheet	3.2	3.2	3.1	2.9
	Barley	2.5	2.4	2.2	2.2
	Cucumber	17.7	16.7	16.1	15.3
	Maize	31.5	31.1	22.7	23.8
	Onion	44.9	42.9	41.3	40.1
	Potato	37.8	35.6	34.6	32.1
	Sugarbeet	33.3	30.8	28.0	27.9
	Tomato	34.1	33.9	32.6	30.2
	Alfalfa	9.2	9.1	9.0	8.6
	Average	23.8	22.9	21.1	20.4
Water requirment	Wheet	5691	7113	7568	7800
	Barley	2601	3405	4075	4102
	Cucumber	11215	13026	15319	17534
	Maize	13941	16452	18114	21022
	Onion	14055	14624	17366	21936
	Potato	15496	19000	23000	29000
	Sugarbeet	16890	17366	19194	21022
	Tomato	12641	14498	16938	16994
	Alfalfa	13269	13714	17499	20198
	Average	11755	13244	15452	17734

594 As demonstrated in Figure 5, among the various crops, potatoes demonstrated the most
595 significant increase in net water requirement, with an 87% surge, while sugar beets exhibited
596 the least substantial increase, with a 24% rise. Furthermore, the smallest and largest declines
597 in yield were observed in alfalfa (6% decrease compared to current conditions) and forage corn
598 (24% decrease compared to current conditions), respectively.

599

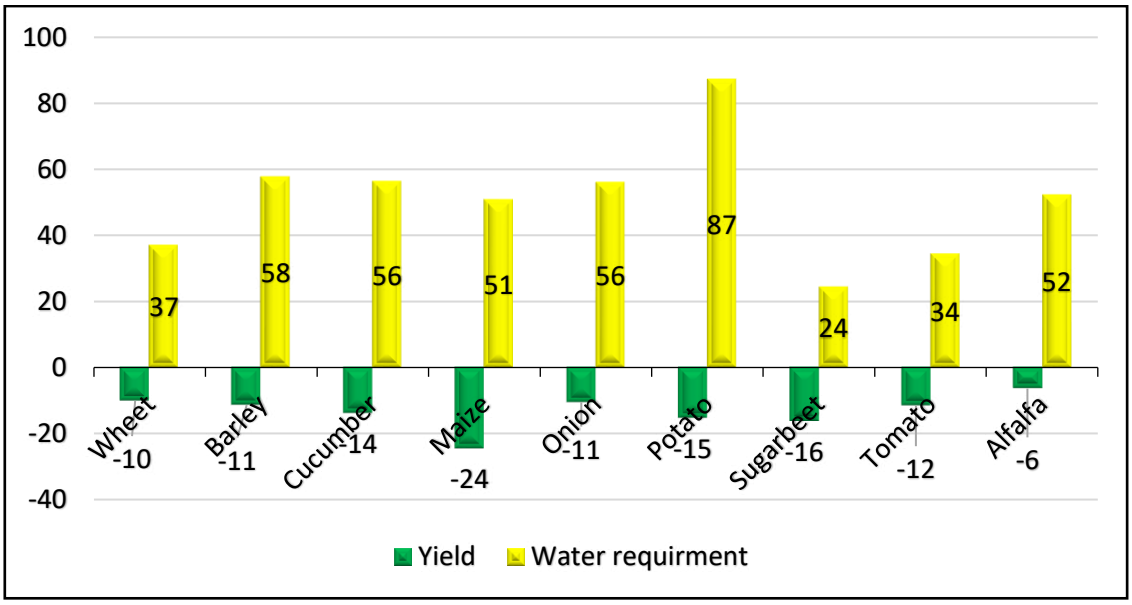
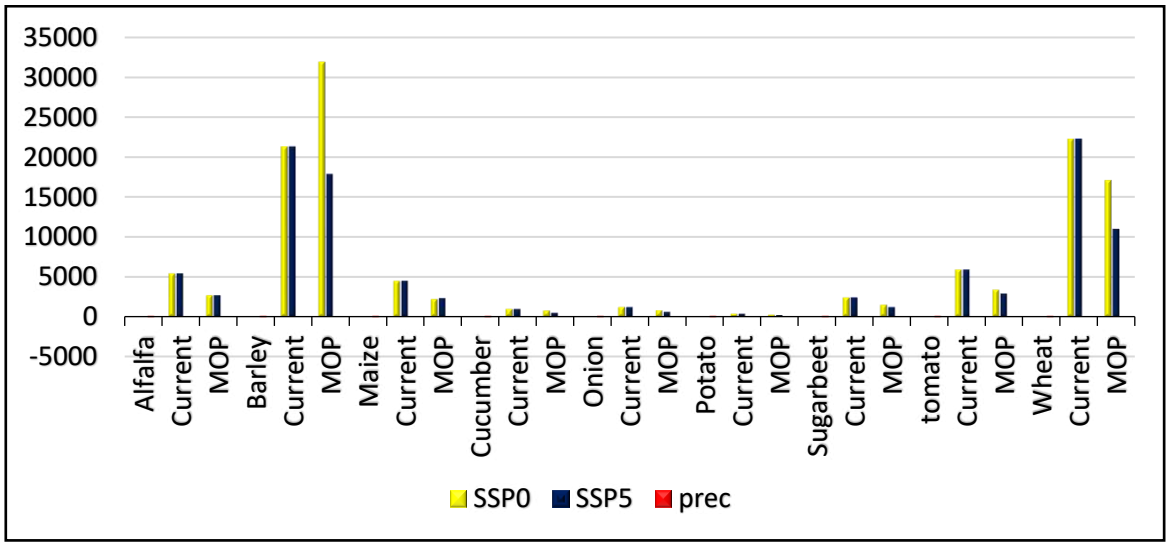


Figure 5. Percentage change in crop yield and net water requirement under climate change conditions.

4.4 Results Interconnectedness of water, energy, and food Modeling

The alterations in cultivated area under the optimal crop pattern scenario, without considering climate change and accounting for changes in yield, water requirements, and water availability under predicted climate change conditions up to 2040, are demonstrated in Figure 6. In the context of climate change, and more specifically within the confines of a pessimistic scenario, the cultivated area for the majority of crops, with the exception of barley, experiences a 50% diminution in comparison to its current state. It is noteworthy that barley exhibits the smallest reduction in cultivated area, with a decrease of only 16% compared to the current level.



611 Figure 6. Comparison of cultivated areas under crop pattern adaptation scenarios and
612 climate change (ha).

613 The key economic variables associated with the scenarios of adapting cultivated area and
614 climate change are reported in Table 7. A review of the extant literature reveals a consensus
615 that climate change conditions result in a decline in costs, fertilizer consumption, pesticide use,
616 greenhouse gas emissions, irrigation water consumption, calorie production, total output, and
617 ultimately the cultivated area of crops when compared to current levels. However, given that
618 one of the primary objectives of the nexus is to enhance economic income and reduce
619 environmental issues, the implementation of climate change scenarios and optimal cropping
620 patterns has led to a reduction in input usage. Conversely, this has resulted in a 25% decrease
621 in farmers' profits, a 40% reduction in cultivated area, a 41% decline in calorie production from
622 crops, a 45% decrease in Water available, and, consequently, food security is severely impacted
623 under climate change conditions. Consequently, in order to align with sustainable development
624 goals and maintain stability in farmers' incomes, it is imperative to seriously consider and
625 implement policies aimed at addressing these challenges.

626 Table 7. Key economic variables based on the water-food-energy nexus approach.

Variables	Current	Optimal	Percentage change
Costs ((million IRR/ha)	48632	17800	-63
Greenhouse gas emissions (Million Tons ha)	206	116	-44
Calories from production (Billion Calories /ha)	830	491	-41
Net profit of farmers (billion IRR/)	40626	30659	-25
Cultivated area (ha)	64006	38920	-40
Water consumption (million cubic meters-hectares)	137.016	634.564	-45

627

628 4.5 Water and Carbon Footprint Assessment

629 The total water footprint for the entire basin under the cultivated area change scenario and the
630 climate change scenario is illustrated in Figure 7. The total water footprint under the cultivated
631 area change scenario is 23,723 million m3, which increases by 58% to 37,513 million m3 under
632 climate change conditions.

633 Conversely, the aggregate green water footprint for the entire basin under the climate change
634 scenario exhibits an augmentation of 11.87% (3,184 million m3) in comparison with the
635 cultivated area change scenario. This finding suggests a heightened reliance on surface and
636 groundwater resources for production in the region under climate change conditions.

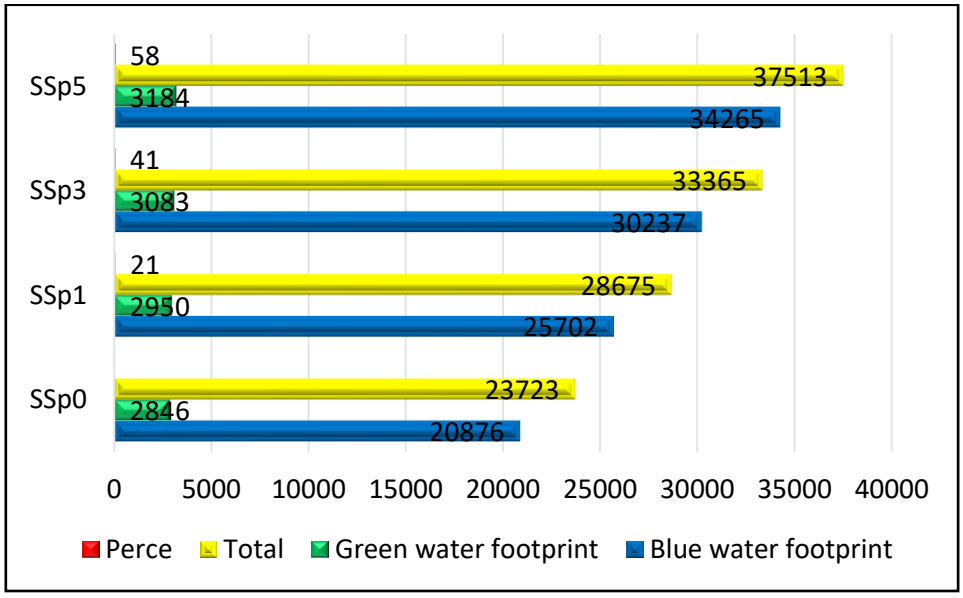


Figure 7. Comparison of blue and green water footprints under adaptation and change scenarios.

The projected carbon footprint of crops under climate change conditions is illustrated in Figure 8. The highest carbon footprints were attributed to barley, sugar beet, forage corn, and tomatoes, respectively, while the lowest carbon footprints were associated with cucumbers, onions, potatoes, alfalfa, and wheat. Notably, the highest projected carbon footprint is predicted for barley, accounting for 20% of the total, while the lowest is projected for wheat, at 4%, by the year 2040.

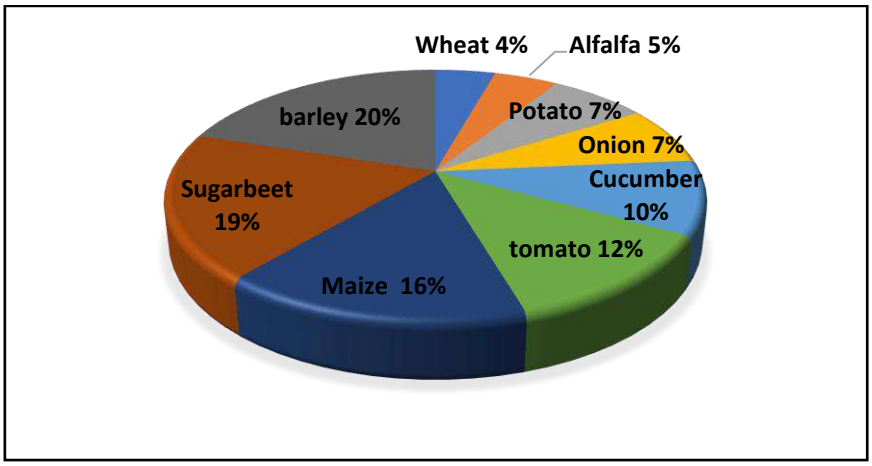


Figure 8. Projected carbon footprint of crops under climate change conditions.

In summary, thus far, the present study has evaluated two scenarios for developing robust adaptation pathways based on the water-energy-food nexus approach. The first scenario

involves changes in crop cultivation patterns. The second scenario is assessed using a multi-objective optimization model. The model is then compared to current conditions.

Given the multifaceted nature of climate change, impacting economic, environmental, and resource consumption, and most critically, food security in various ways, the study further proposes an additional key adaptation strategy to address the consequences and damages caused by this phenomenon, tailored to the basin's specific conditions. This strategy entails enhancing the efficacy of irrigation systems in agricultural fields by 10%. The implementation of this measure is expected to yield a number of favorable outcomes, including the sustained cultivation of crop areas, improved farmer profits, reduced costs, and optimized resource use for farmers and stakeholders in the basin.

4.6 Results of Water-Food-Energy Nexus Modeling with Improved Irrigation Efficiency

The alterations in cultivated area subsequent to the implementation of the irrigation efficiency enhancement policy, in comparison with climate change conditions, are illustrated in Figure 9. Among the crops examined, wheat and barley, which occupy the most extensive cultivated areas in the basin, exhibited reductions of 51% and 16%, respectively, under the climate change scenario. However, with the implementation of enhanced irrigation techniques, the cultivated area for these crops exhibited a substantial increase of 26% and 6%, respectively, in comparison to conditions influenced by climate change. Furthermore, the cultivated area for other crops, including forage corn, onions, and alfalfa, exhibited a marginal increase in this scenario, averaging 1–2% compared to conditions under climate change.

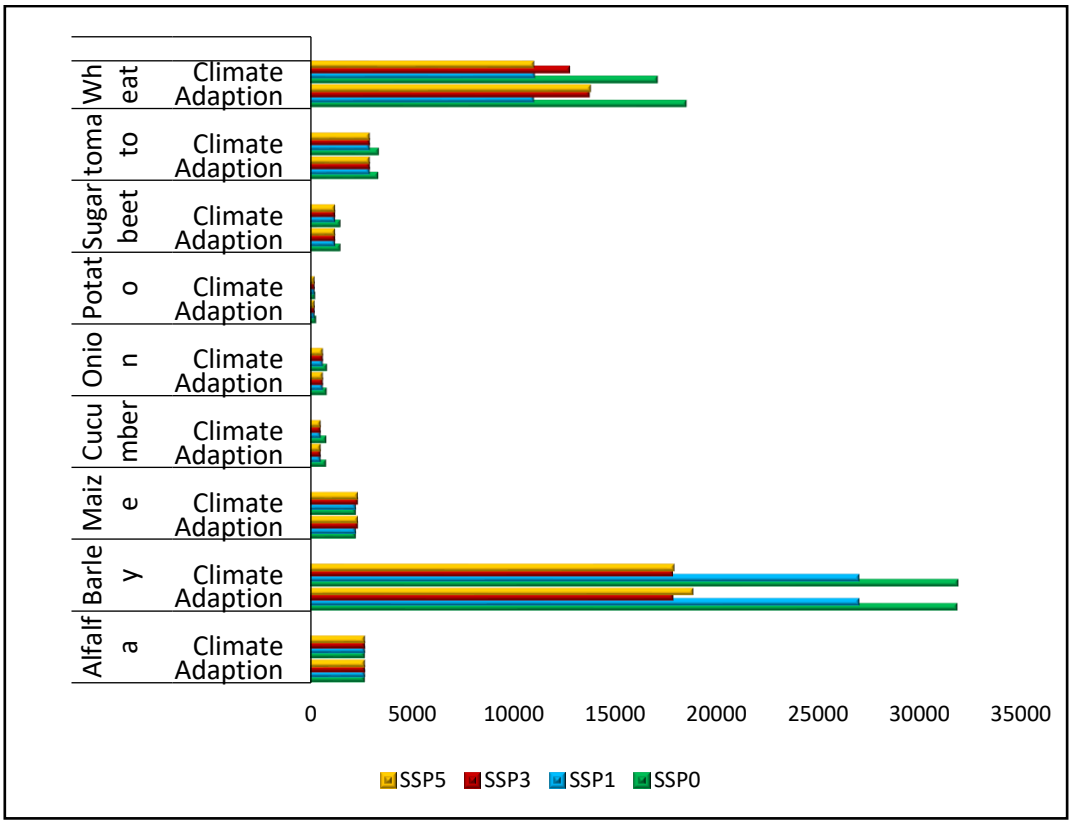


Figure 9. Changes in cultivated area under climate change and adaptation scenarios.

According to the explanations that have been provided, from an economic perspective, the improvement of irrigation efficiency as an adaptation strategy has been shown to be partially effective in mitigating the reduction in cultivated area under climate change conditions. This strategy is designed to enhance farmers' income stability and control costs, as illustrated in Figure 10. Consequently, the farmers' net profit exhibited a 39% increase under the cultivated area change scenario. Conversely, under conditions of climate change, net profit exhibits a 24% decrease in comparison with the scenario of crop pattern change. Consequently, the implementation of the proposed adaptation strategy to support farmers has been shown to result in a relatively significant increase in net profit of 33,115 million rials (8%) under the pessimistic scenario compared to conditions of climate change. However, this trend remains largely unchanged for optimistic and moderate scenarios. Furthermore, under conditions of climate change, the application of a water-energy-food nexus approach has been demonstrated to result in a 63% reduction in costs. Conversely, the implementation of policies aimed at enhancing irrigation efficiency can result in a marginal 4% increase in costs under climate change conditions. This is due to the fact that the execution of any policy necessitates additional expenses, including the adoption of technology, its promotion, training, and associated measures.

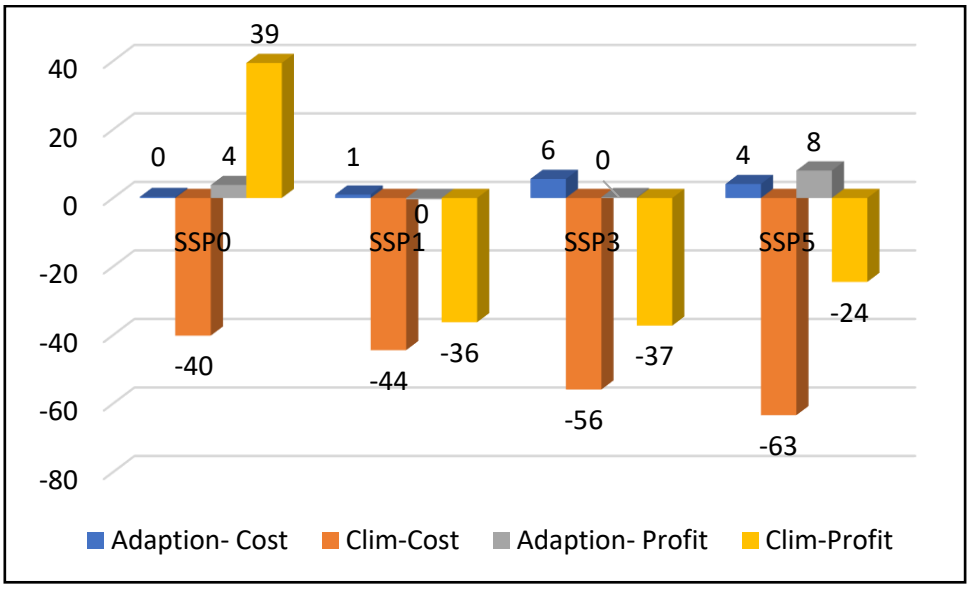


Figure 10. Comparison of farmers' net profit and total consumption costs under climate change and adaptation scenarios.

5 Discussion

The findings of this study reveal complex, non-linear interactions across the hydrological, environmental, and economic dimensions of the WEF nexus. Rather than merely reporting scenario outcomes, this discussion elucidates the underlying causal mechanisms, quantifies critical policy trade-offs, examines uncertainty propagation, and contrasts systemic feedbacks with prior literature. The analysis demonstrates that climate-induced stresses propagate asymmetrically through the nexus, creating distinct leverage points for adaptation while exposing inherent conflicts between resource conservation, economic viability, and emission reduction targets.

5.1 Hydrological Dimension

The projected 20% decline in aggregate crop yields and 15% increase in net irrigation requirements under SSP5 are not merely functions of altered precipitation totals, but stem from two compounding hydroclimatic mechanisms. First, a 6.95°C rise in monthly maximum temperatures directly amplifies reference evapotranspiration (ET_0), accelerating soil moisture depletion and elevating crop water stress. Second, the temporal redistribution of rainfall—despite statistically insignificant annual changes—disrupts critical phenological windows, particularly during reproductive stages. This mechanism explains the asymmetric vulnerability observed across crops: silage corn exhibits a 24% yield reduction compared to only 6% for alfalfa, reflecting corn's higher thermal sensitivity and narrower optimal temperature window during tasseling and grain filling. From a systemic perspective, this hydrological stress propagates directly into the energy and food dimensions by forcing farmers to extract deeper groundwater or shift to less water-intensive but lower-yielding crops. Policy implications are twofold: (i) climate-resilient cropping patterns must prioritize phenological thermal tolerance over static water requirements, and (ii) irrigation scheduling must adapt to intra-seasonal

rainfall variability rather than annual averages. Notably, model sensitivity analyses indicate that a 10% uncertainty in precipitation timing propagates nonlinearly, amplifying yield variability by up to 18%, underscoring the need for dynamic, rather than fixed, water allocation frameworks. These findings contrast with Ahani et al. (2024) and Kalbali et al. (2021), who treated climate impacts as uniform reductions in water availability, thereby overlooking crop-specific phenological thresholds that critically modulate hydrological stress into economic and nutritional outcomes.

5.2 Environmental Dimension

The integrated adaptation strategy achieves a 44% reduction in basin-level greenhouse gas (GHG) emissions, yet this environmental gain emerges from a pronounced economic-hydrological trade-off. Barley, which accounts for 20% of the baseline carbon footprint, retains a significant share of the optimized cropping pattern. This counterintuitive outcome is mechanistically driven by water scarcity: under severe deficit conditions, barley delivers a higher marginal profit per unit of water consumed compared to wheat. Consequently, aggressively displacing barley to lower emissions would paradoxically destabilize farm incomes and trigger compensatory land-use changes that could increase regional emissions elsewhere. This reveals a fundamental WEF nexus trade-off: immediate water security and economic viability often constrain the feasibility of stringent decarbonization pathways. From a policy standpoint, this necessitates a tiered intervention approach. Short-term measures should focus on optimizing irrigation efficiency and shifting to low-water, low-carbon crops (e.g., alfalfa, wheat, onions), while long-term climate commitments require targeted carbon pricing or subsidies to decouple barley cultivation from high-emission practices. The environmental benefits observed here are highly sensitive to carbon footprint coefficients; a ±15% variation in emission factors propagates to a 22–28% uncertainty in total GHG reduction, highlighting the need for localized, crop-specific life-cycle assessment data. Unlike studies that treat environmental and economic objectives as sequentially achievable (e.g., Li et al., 2019), our results demonstrate that simultaneous WEF optimization requires explicit constraint relaxation and compensatory mechanisms, as rigid emission targets without economic buffers risk exacerbating water poverty and reducing adaptive capacity.

5.3 Economic Dimension

Economically, a 10% improvement in irrigation efficiency serves as the most potent adaptation lever, fully offsetting the 24% profit decline projected under unmitigated climate change and generating an 8% net profit increase relative to baseline conditions. The underlying mechanism is not merely yield preservation, but hydrological reallocation: water savings from efficiency gains are strategically redirected to expand cultivated areas, particularly for drought-tolerant cereals. Although the capital investment incurs a 4% operational cost premium, this is rapidly amortized by the 8% gross revenue uplift, yielding a 3–5 year payback period. Critically, financial viability is highly contingent on institutional support; a 30% public subsidy for pressurized irrigation infrastructure compresses the payback horizon to ~2 years, transforming the technology from a capital-intensive risk to an accessible adaptation pathway for

smallholders. However, one-at-a-time (OAT) sensitivity analysis reveals profound economic uncertainty propagation: a 10% reduction in water availability triggers a 28% profit contraction, while a 5% yield decline reduces profits by 22%. This asymmetry confirms that hydrological uncertainty dominates economic risk, and efficiency gains alone cannot compensate for systemic water depletion without complementary governance reforms. These findings fundamentally diverge from prior hydro-economic applications (e.g., Esteve et al., 2015; Li et al., 2019), which typically model economic optimization as a unidirectional driver, treating environmental outcomes as secondary by-products. In contrast, our coupled nexus framework reveals that ignoring bidirectional feedbacks—such as temperature-driven yield declines simultaneously reducing water demand but increasing extraction costs—systematically overestimates economic resilience by 15–20% and underestimates climate vulnerability. Consequently, policy design must shift from isolated technological interventions to integrated resource governance that aligns water pricing, subsidy structures, and carbon accounting to navigate the inherent trade-offs between profitability, equity, and sustainability.

5.4 Summary and Hypothesis Assessment

Table 8 presents the key hypotheses of the current study and their empirical validation. The results project a basin-wide decline in crop yields by 2040 due to changing climatic conditions, with the most pronounced reductions observed in forage crops—a finding consistent with Esteve et al. (2015) in the Guadiana Basin and Li et al. (2019) in the Heihe River Basin. Specifically, forage maize exhibits the largest yield reduction (16%), whereas alfalfa shows the smallest decline (8%). The analysis further reveals a positive correlation between rising temperatures, increased crop water demand, and reduced yields, thereby supporting the first hypothesis.

Climate change is projected to reduce basin-scale water availability by approximately 20%, confirming the second hypothesis. In the absence of adaptation measures, Mardani Najafabadi et al. (2019) estimated a 10% contraction in cultivated area across several Iranian regions, including Isfahan Province. In contrast, the present study demonstrates that implementing targeted adaptation policies could expand the cultivated area by up to 15% under climate change scenarios.

The third hypothesis is corroborated by the projected decline in the optimal allocation of cultivated land in the Karkheh River Basin under climate stress. Furthermore, the fourth hypothesis is validated through the finding that adaptation policies can reduce greenhouse gas emissions by 44% under climate change conditions, highlighting their dual role in enhancing agricultural resilience and mitigating environmental impacts.

Finally, under hydroclimatic variability, farmers' net income is projected to decline by 24%. However, the proposed adaptation strategies—centered on optimized resource allocation—can increase net profitability by up to 8%, thereby confirming the fifth hypothesis and underscoring the socio-economic efficacy of integrated adaptation planning.

Table 8. Key Assumptions of the Research

Row	Hypothesis	Evaluation
1	climate change will reduce crop yields and increase water requirements in the Kashfarud River basin.	✅
2	climate change will reduce the water resources available to the agricultural sector in the Kashfarud River basin.	✅
3	climate change will lead to a decrease in the optimal area of agricultural land in the Kashfarud River basin.	✅
4	climate change adaptation policies can reduce greenhouse gas emissions.	✅
5	these policies will lead to an increase in farmers' income within the framework of optimal resource allocation.	✅

5.5 Contextualized Transferability Framework

While the proposed WEF-hydroeconomic framework demonstrates structural adaptability, its transferability to other arid basins is inherently conditional upon institutional, socio-economic, and infrastructural heterogeneity. Direct scalability is neither feasible nor scientifically defensible, as water governance regimes, subsidy structures, data availability, and irrigation infrastructure maturity vary substantially across regions. Instead, the model employs a modular architecture that enables context-sensitive recalibration: (i) hydrological modules can be re-parameterized using locally calibrated crop coefficients and basin-specific climate projections; (ii) economic constraints can be adjusted to reflect regional water pricing, land tenure systems, and fiscal capacity; and (iii) policy scenarios must be redesigned to align with institutional enforcement capabilities and socio-political acceptance thresholds. Consequently, the framework should be viewed as a decision-support template rather than a plug-and-play solution, requiring localized data integration, stakeholder co-design, and phased implementation pathways to ensure policy relevance and operational feasibility.

5.6 Limitations and Future Research

Implementing water–energy–food (WEF) nexus strategies for sustainable development requires advanced technologies and institutional innovation. However, this study faced several limitations. First, limited coordination among relevant organizations hindered integrated planning. Second, there is a notable lack of awareness and reliable data on energy, water, and food consumption across sectors. Third, sector-specific challenges remain poorly defined.

To effectively regulate greenhouse gas emissions in agriculture and recognize the critical role of energy carriers, future efforts must prioritize: (i) the type and quantity of energy inputs, and (ii) the nature and volume of agricultural inputs used.

Substantial emission reductions will depend on improving energy efficiency across crops and replacing fossil fuels with renewable energy sources. Accordingly, future research should focus on three key areas:

- Developing integrated frameworks for cross-sectoral data collection and institutional collaboration;
- Assessing the economic and environmental feasibility of clean energy adoption in agriculture;
- Designing policy incentives to foster technological innovation and stakeholder coordination.

This study identifies the creation of specialized nexus-oriented enterprises as a critical enabler of systemic transformation. Scaling such technological frameworks requires robust institutional arrangements for policy formulation and multi-sectoral alignment. For instance, coordinated action among the Ministries of Energy, Agriculture, Industry and Mining, and the National Water Organization would be instrumental in achieving shared objectives.

Moreover, integrating comprehensive energy modeling tools—such as the Long-range Energy Alternatives Planning (LEAP) system with water resource models like WEAP would enable simultaneous simulation of energy and water dynamics at the basin scale.

Finally, to address the inherent uncertainties in agricultural systems, we recommend incorporating advanced optimization techniques such as robust optimization (RO) into the nexus modeling framework. Novel approaches, including fuzzy decision-making, multi-criteria analysis, and metaheuristic algorithms, offer promising avenues for enhancing model robustness. Specifically, a fuzzy-based water–food–energy coupling framework under simulated climate scenarios could enable precise evaluation of irrigation networks and strengthen the operationalization of the WEF nexus strategy.

6 Conclusion

This study represents a pioneering step toward integrating multi-objective hydrological, environmental, and economic models into a unified framework for optimizing crop patterns in the Kashafrud River Basin. The proposed Hydro-Economic-Environmental Model (HEEM) effectively balances competing objectives economic profitability, resource efficiency, and environmental protection by enabling the optimal allocation of agricultural inputs, including irrigation water, pesticides, and chemical fertilizers, under diverse climate change and adaptation scenarios. Application of the HEEM framework enhances farmers' gross profits while strengthening the resilience of agricultural systems to climatic variability. Notably, policies targeting improved irrigation efficiency implemented through this model yield significant reductions in both water consumption and greenhouse gas emissions, demonstrating its dual economic and environmental sustainability. From a policy standpoint, the findings highlight the benefits of adopting optimized cropping patterns and resource-efficient practices, which can stabilize farm incomes and bolster climate resilience. To scale these solutions, governments must establish supportive institutional frameworks that incentivize adoption and facilitate knowledge transfer. Concurrently, water resource managers should implement

integrated, data-driven strategies to ensure the sustainable use and conservation of basin water resources. Ultimately, this integrative approach provides a robust scientific foundation for advancing climate-resilient agriculture, promoting environmental stewardship, and enhancing regional food self-sufficiency.

Declaration of interests

- **Ethics approval and consent to participate**

Not applicable. This study did not involve human participants, animals, or biological materials.

- **Consent for publication**

Not applicable. The manuscript does not contain any individual person's data.

- **Competing Interests**

The authors declare that they have no known competing financial interests or personal relationships that could have appeared to influence the work reported in this paper.

- **Funding**

This research did not receive any specific grant from funding agencies in the public, commercial, or not-for-profit sectors.

Data Availability

The data supporting this study's findings are openly available in [Mendeley Data] at V1 [DOI: 10.17632/xxgf37bbcf.1] under the reference number [https://data.mendeley.com/datasets/xxgf37bbcf/1].

AI Use Disclosure

Generative AI tools were used solely for translation and language polishing; all authors retain full responsibility for the scientific content, accuracy, and final version of this manuscript.

References

FAO. (2008). AQUASTAT Country Profile – Iran (Islamic Republic of). *Food and Agriculture Organization of the United Nations, Rome*. https://www.fao.org/aquastat/en/countries-and-basins/country-profiles/country/IRN/

Al-Saidi, M., & Elagib, N. A. (2017). Towards understanding the integrative approach of the water, energy, and food nexus. *Science of The Total Environment*, *574*, 1131–1139. https://doi.org/https://doi.org/10.1016/j.scitotenv.2016.09.046

Ahani, E., Ziaee, S., Mohammadi, H., Mardani Najafabadi, M., & Mirzaei, A. (2024). An Investigation into the Effects of Climate Change on Water–Energy–Food Nexus: A New Mathematical Programming Approach. *International Journal of Environmental Research*, Volume 18, Issue 2. https://doi.org/https://doi.org/10.1007/s41742-024-00567-9

Cao, X., Bao, Y., Li, Y., Li, J., & Wu, M. (2023). Unravelling the effects of crop blue, green, and grey virtual water flows on regional agricultural water footprint and scarcity. *Agricultural Water Management*, *278*, 108165. https://doi.org/https://doi.org/10.1016/j.agwat.2023.108165

Cao, X., Zeng, W., Wu, M., Guo, X., & Wang, W. (2020). Hybrid analytical framework for regional agricultural water resource utilization and efficiency evaluation. *Agricultural Water Management*, *231*, 106027. https://doi.org/https://doi.org/10.1016/j.agwat.2020.106027

Chen, S., & Chen, B. (2016). Urban energy–water nexus: A network perspective. *Applied Energy*, *184*, 905–914. https://doi.org/https://doi.org/10.1016/j.apenergy.2016.03.042

Deng, X., & Gibson, J. (2019). Improving eco-efficiency for the sustainable agricultural production: A case study in Shandong, China. *China. Technological Forecasting and Social Change*, *14*(4), 394-400.

EL-Gafy, I., Grigg, N., & Waskom, R. (2017). Water-Food-Energy: Nexus and Non-Nexus Approaches for Optimal Cropping Pattern. *Water Resources Management*, *31*(15), 4971–4980. https://doi.org/10.1007/s11269-017-1789-0

Emamzadeh, S. M., Forghani, M. A., Karnema, A., & Darbandi, S. (2016). Determining an optimum pattern of mixed planting from organic and non-organic crops with regard to economic and environmental indicators: A case study of cucumber in Kerman, Iran. *Information Processing in Agriculture*, *3*(4), 207–214. https://doi.org/https://doi.org/10.1016/j.inpa.2016.08.001

Esteve, P., Varela-Ortega, C., Blanco-Gutiérrez, I., & Downing, T. E. (2015). A hydro-economic model for the assessment of climate change impacts and adaptation in irrigated agriculture. *Ecological Economics*, *120*, 49–58. https://doi.org/https://doi.org/10.1016/j.ecolecon.2015.09.017

Fabiani, S., Vanino, S., Napoli, R., & Nino, P. (2020). Water energy food nexus approach for sustainability assessment at farm level: An experience from an intensive agricultural area in central Italy. *Environmental Science & Policy*, *104*, 1–12. https://doi.org/https://doi.org/10.1016/j.envsci.2019.10.008

Han, Y., Xu, Y., Cao, R., & Liu, Z. (2024). Optimization framework for eco-hydrological connectivity schemes based on graph theory and waterfront accessibility. *Journal of Hydrology: Regional Studies*, *56*, 101975.

https://doi.org/https://doi.org/10.1016/j.ejrh.2024.101975

Ikram, M., Zhang, Q., Sroufe, R., & Shah, S. Z. A. (2020). Towards a sustainable environment: The nexus between ISO 14001, renewable energy consumption, access to electricity, agriculture, and CO2 emissions in SAARC countries. *Sustainable Production and Consumption*, *22*, 218–230. https://doi.org/https://doi.org/10.1016/j.spc.2020.03.011

Jones, E. C., & Leibowicz, B. D. (2022). Climate risk management in agriculture using alternative electricity and water resources: a stochastic programming framework. *Environment Systems and Decisions,* *42*(1), 117–135. https://doi.org/https://doi.org/10.1007/s10669-021-09838-8

Kalbali, E., Ziaee, S., Najafabadi, M. M., & Zakerinia, M. (2021). Approaches to adapting to impacts of climate change in northern Iran: The application of a Hydrogy-Economics model. *Journal of Cleaner Production*, *280*, 124067. https://doi.org/https://doi.org/10.1016/j.jclepro.2020.124067

Karanisa, T., Achour, Y., Ouammi, A., & Sayadi, S. (2022). Smart greenhouses as the path towards precision agriculture in the food-energy and water nexus: case study of Qatar. *Environment Systems and Decisions,* *42*(4), 521–546. https://doi.org/https://doi.org/10.1007/s10669-022-09862-2

Keating, B. A., Carberry, P. S., Bindraban, P. S., Asseng, S., Meinke, H., and Dixon, J. (2010). Eco-efficient agriculture: Concepts, challenges, and opportunities. *Crop Science.*, *50*(S1), S-109-S-119.

Kurian, M. (2017). The water-energy-food nexus: Trade-offs, thresholds and transdisciplinary approaches to sustainable development. *Environmental Science & Policy*, *68*, 97–106. https://doi.org/https://doi.org/10.1016/j.envsci.2016.11.006

Lalawmpuii, & Rai, P. K. (2023). Role of water-energy-food nexus in environmental management and climate action. *Energy Nexus*, *11*, 100230. https://doi.org/https://doi.org/10.1016/j.nexus.2023.100230

Li, M., Fu, Q., Singh, V. P., Ji, Y., Liu, D., Zhang, C., & Li, T. (2019). An optimal modelling approach for managing the agricultural water-energy-food nexus under uncertainty. *Science of The Total Environment*, *651*, 1416–1434. https://doi.org/https://doi.org/10.1016/j.scitotenv.2018.09.291

Li, M., Fu, Q., Singh, V. P., Ma, M., & Liu, X. (2017). An intuitionistic fuzzy multi-objective non-linear programming model for sustainable irrigation water allocation under the combination of dry and wet conditions. *Journal of Hydrology*, *555*, 80–94. https://doi.org/https://doi.org/10.1016/j.jhydrol.2017.09.055

Liu, Y., Wang, S., & Chen, B. (2017). Regional water–energy–food nexus in China based on multiregional input–output analysis. *Energy Procedia*, *142*, 3108–3114. https://doi.org/https://doi.org/10.1016/j.egypro.2017.12.452

Lodge, J. W., Dansie, A. P., & Johnson, F. (2023). A review of globally available data sources

for modelling the Water-Energy-Food Nexus. *Earth-Science Reviews*, *243*, 104485. https://doi.org/https://doi.org/10.1016/j.earscirev.2023.104485

Lu, S., Zhang, X., Peng, H., Skitmore, M., Bai, X., & Zheng, Z. (2021). The energy-food-water nexus: Water footprint of Henan-Hubei-Hunan in China. *Renewable and Sustainable Energy Reviews*, *135*, 110417. https://doi.org/https://doi.org/10.1016/j.rser.2020.110417

Madani, K., AghaKouchak, A., Mirchi, A. (2016). Iran's Socio-economic Drought: Challenges of a Water-Bankrupt Nation. *Iranian Studies*, *49*(6), 997–1016.

Mardani Najafabadi, M., Ziaee, S., Nikouei, A., & Ahmadpour Borazjani, M. (2019). Mathematical programming model (MMP) for optimization of regional cropping patterns decisions: A case study. *Agricultural Systems*, *173*, 218–232. https://doi.org/https://doi.org/10.1016/j.agsy.2019.02.006

Mohamad Arbai, N. A., & Irie, M. (2025). Effects of climate change on wet and dry spells in the Kelantan River basin using a physically-based hydrological model and CMIP6 scenarios. *Journal of Hydrology: Regional Studies*, *58*, 102219. https://doi.org/https://doi.org/10.1016/j.ejrh.2025.102219

Motta, C., Naumann, G., Gomez, D., Formetta, G., & Feyen, L. (2025). Assessing the economic impact of droughts in Europe in a changing climate: A multi-sectoral analysis at the regional scale. *Journal of Hydrology: Regional Studies*, *59*, 102296. https://doi.org/https://doi.org/10.1016/j.ejrh.2025.102296

Nabavi-Pelesaraei, A., Rafiee, S., Hosseinzadeh-Bandbafha, H., & Shamshirband, S. (2016). Modeling energy consumption and greenhouse gas emissions for kiwifruit production using artificial neural networks. *Journal of Cleaner Production*, *133*, 924–931. https://doi.org/https://doi.org/10.1016/j.jclepro.2016.05.188

Nie, Y., Avraamidou, S., Xiao, X., Pistikopoulos, E. N., Li, J., Zeng, Y., Song, F., Yu, J., & Zhu, M. (2019). A Food-Energy-Water Nexus approach for land use optimization. *Science of The Total Environment*, *659*, 7–19. https://doi.org/https://doi.org/10.1016/j.scitotenv.2018.12.242

Peng, W., Zheng, H., Robinson, B. E., Li, C., & Li, R. (2022). Comparing the importance of farming resource endowments and agricultural livelihood diversification for agricultural sustainability from the perspective of the food–energy–water nexus. *Journal of Cleaner Production*, *380*, 135193. https://doi.org/10.1016/J.JCLEPRO.2022.135193

Puchongkawarin, C. (2024). Enviro-economic optimization for the design of municipal solid waste management strategies. *Environment Systems and Decisions, 44*(3), 674–694. https://doi.org/https://doi.org/10.1007/s10669-024-09963-0

Rezaei Zaman, M., Morid, S., & Delavar, M. (2016). Evaluating climate adaptation strategies on agricultural production in the Siminehrud catchment and inflow into Lake Urmia, Iran, using SWAT within an OECD framework. *Agricultural Systems*, *147*, 98–110. https://doi.org/https://doi.org/10.1016/j.agsy.2016.06.001

Teutschbein, C., Jonsson, E., Todorović, A., Tootoonchi, F., Stenfors, E., & Grabs, T. (2023). Future drought propagation through the water-energy-food-ecosystem nexus – A Nordic perspective. *Journal of Hydrology*, *617*, 128963. https://doi.org/10.1016/j.jhydrol.2022.128963

Wang, X., Fielding, K. S., & Dean, A. J. (2023). "Nature is mine/ours": Measuring individual and collective psychological ownership of nature. *Journal of Environmental Psychology*, *85*, 101919. https://doi.org/https://doi.org/10.1016/j.jenvp.2022.101919

Wu, L., Elshorbagy, A., & Alam, M. S. (2022). Dynamics of water-energy-food nexus interactions with climate change and policy options. *Environmental Research Communications*, *4*(1), 15009. https://doi.org/10.1088/2515-7620/ac4bab

Yue, Q., & Guo, P. (2021). Managing the agricultural water-energy-food-environment nexus considering water footprint and carbon footprint under uncertainty. *Agricultural Water Management*, *252*, 106899. https://doi.org/https://doi.org/10.1016/j.agwat.2021.106899

Zhang, X., & Vesselinov, V. V. (2016). Energy-water nexus: Balancing the tradeoffs between two-level decision makers. *Applied Energy*, *183*, 77–87. https://doi.org/https://doi.org/10.1016/j.apenergy.2016.08.156

Figures



Figure 1

Monthly Maximum Temperature Changes for the Period 2021–2040 Compared to the Baseline Period


Figure 2

Verification and validation of water requirement and crop yield parameters


Figure 3

Percentage change in crop yield and net water requirement under climate change conditions.


Figure 4

Comparison of cultivated areas under crop pattern adaptation scenarios and climate change (ha).


Figure 5

Comparison of blue and green water footprints under adaptation and change scenarios.


Figure 6

Projected carbon footprint of crops under climate change conditions.


Figure 7

Changes in cultivated area under climate change and adaptation scenarios.


Figure 8

Comparison of farmers' net profit and total consumption costs under climate change and adaptation scenarios.